

CHEMICAL REVIEWS

Mechanism of Nitrogen Fixation by Nitrogenase: The Next Stage

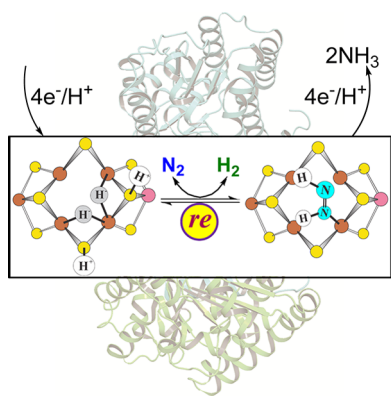
Brian M. Hoffman,*[§] Dmitriy Lukyanov,[§] Zhi-Yong Yang,[†] Dennis R. Dean,*[‡] and Lance C. Seefeldt*,[†]

[†]Department of Chemistry and Biochemistry, Utah State University, 0300 Old Main Hill, Logan, Utah 84322, United States

[‡]Department of Biochemistry, Virginia Tech, 900 West Campus Drive, Blacksburg, Virginia 24061, United States

[§]Departments of Chemistry and Molecular Biosciences, Northwestern University, 2145 Sheridan Road, Evanston, Illinois 60208, United States

Supporting Information



CONTENTS

1. Introduction	4041
2. Background	4043
2.1. Kinetics and Stoichiometry	4043
2.2. Trapping and Characterization of Substrates	4044
3. Intermediates of Nitrogenase Activation	4044
3.1. E ₁ –E ₃	4044
3.2. E ₄ : The “Janus Intermediate”	4044
3.3. Redox Behavior and Hydride Chemistry of E ₁ –E ₃ : Why Such a Big Catalytic Cluster?	4046
3.4. Why Does Nitrogenase Not React with H ₂ /D ₂ /T ₂ in the Absence of N ₂ ?	4047
4. “Dueling” N ₂ Reduction Pathways	4047
5. Intermediates of N ₂ Reduction: E _n , n ≥ 4	4048
5.1. Intermediate I	4048
5.2. Nitrogenase Reaction Pathway: D versus A	4048
5.3. Intermediate H	4049
6. Unification of the Nitrogenase Reaction Pathway with the LT Kinetic Scheme	4050
7. Obligatory Evolution of H ₂ in Nitrogen Fixation: Reductive Elimination of H ₂	4050
7.1. Hydride Protonation (hp) Mechanism	4051
7.2. Reductive Elimination (re) Mechanism	4051
7.3. Mechanistic Constraints Reveal That Nitrogenase Follows the re Mechanisms	4051
8. Test of the re Mechanism	4052
8.1. Predictions	4053
8.2. Testing the Predictions	4053
9. Completing the Mechanism of Nitrogen Fixation	4054
9.1. Uniqueness of N ₂ and Nitrogenase	4055

9.2. Structure of the E ₄ (N ₂) Intermediate: Some Implications	4056
10. Summary of Mechanistic Insights	4056
10.1. Catalytic Intermediates of N ₂ Fixation	4056
10.2. re Mechanism	4056
10.3. Turnover under N ₂ /D ₂ /C ₂ H ₂ as a Test of the re Mechanism	4057
11. Conclusions	4057
Associated Content	4057
Supporting Information	4057
Author Information	4057
Corresponding Authors	4057
Notes	4058
Biographies	4058
Acknowledgments	4058
References	4058

1. INTRODUCTION

Nitrogen is an essential element contained in many biomolecules necessary to sustain life.^{1,2} This element is abundantly available in Earth’s atmosphere in the form of dinitrogen (N₂) gas, yet most organisms are unable to metabolize N₂ because it is relatively inert.^{3,4} Instead most organisms must obtain their N from “fixed” forms such as ammonia (NH₃) or nitrate (NO₃⁻).^{5–7} Because fixed forms of N are continuously sequestered into sediments, rendering them unavailable for metabolism, and because they are also continuously converted to N₂ through the combined processes of nitrification and denitrification, life can only be sustained by conversion of N₂ to NH₃.^{6,7} This latter process is known as N₂ fixation⁸ and is a critical step in the biogeochemical N cycle.^{5,7,9} N₂ fixation occurs in three different ways: (i) through geochemical processes such as lightning,⁹ (ii) biologically through the action of the enzyme, nitrogenase,^{10,11} found only in a select group of microorganisms,^{12,13} and (iii) industrially through the Haber–Bosch process.^{2,14,15} From the evolution of nitrogenase, approximately two billion years ago¹⁶ until the widespread use of the Haber–Bosch process in the 1950s, all life derived N from biological nitrogen fixation, with geochemical processes representing a minor contributor to the

Special Issue: 2014 Bioinorganic Enzymology

Received: November 5, 2013

Published: January 27, 2014

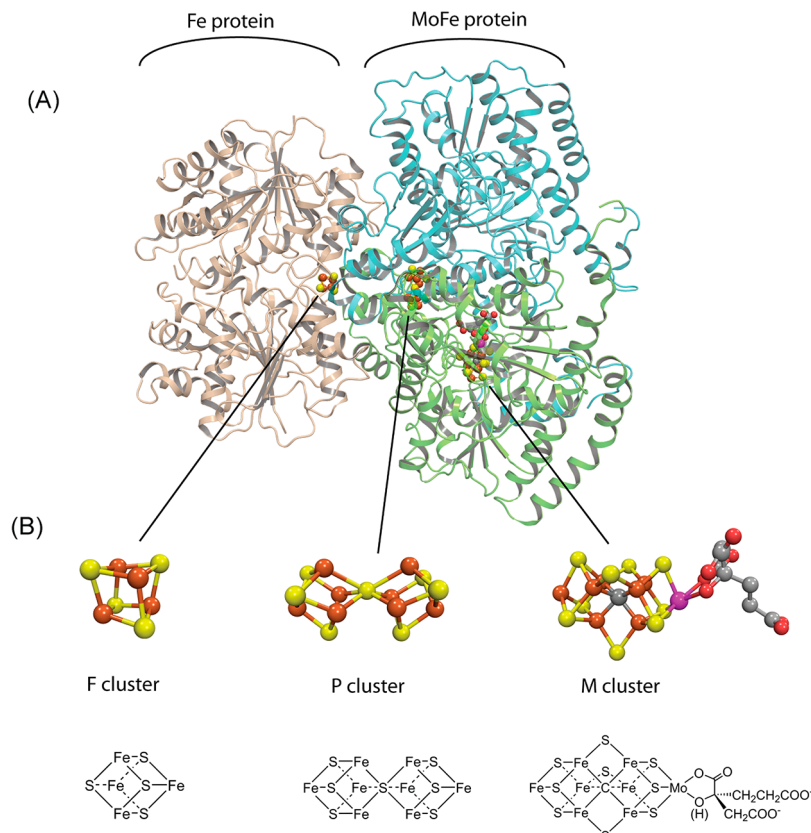


Figure 1. Molybdenum nitrogenase. (A) One catalytic half of the Fe protein:MoFe protein complex with the Fe protein homodimer shown in tan, the MoFe protein α subunit in green, and the β subunit in cyan. (B) Space filling and stick models for the 4Fe–4S cluster (F), P-cluster (P), and FeMo-co (M). Made with Pymol and ChemDraw using PDB:2AFK.

supply of fixed nitrogen.^{2,7} Since the increase in use of the Haber–Bosch process, the biological and industrial processes contribute comparably to N₂ fixation.^{5,7,9}

Nitrogen fixation has a profound agronomic, economic, and ecological impact owing to the fact that the availability of fixed nitrogen represents the factor that most frequently limits agricultural production throughout the world.² Indeed, nearly half of the existing human population could not exist without application of the Haber–Bosch process for production of nitrogen fertilizers.^{2,5} Given that over half of the fixed nitrogen input that sustains Earth's population is supplied biologically, there has been intense interest in understanding how the nitrogenase enzyme accomplishes the difficult task of N₂ fixation at ambient temperature and pressure.^{17,18} An understanding of biological N₂ fixation may further serve as the foundation for achieving two highly desirable, although so far unmet, goals: genetically endowing higher plants with the capacity to fix their own nitrogen,^{19–21} and developing improved synthetic catalysts based on the biological mechanism.^{3,4,22–25}

It has been over 150 years since Jodin first suggested that microbes could “fix” N₂,²⁶ and more than a century since the first isolation of N₂-fixing bacteria around 1900. In 1934, Burk coined the term “nitrogenase”,^{10,11} for the enzyme that catalyzes the conversion of N₂ to a bioaccessible form of nitrogen, and initiated the first meaningful studies of nitrogenase in living cells. Methods for extracting nitrogenase in an active form were developed in the early 1960s,^{27–29} opening the way for serious mechanistic investigations. The next 35 years witnessed intensive efforts by numerous investigators to reveal the

structure and catalytic function of nitrogenase.^{30–34} These developments were summarized in the magisterial review by Burgess and Lowe in 1996.¹⁷ Key advances in understanding nitrogenase structure and function during those intervening years included the following: (i) It was determined that nitrogenase is a two-component system^{35–37} composed of the MoFe protein (also called dinitrogenase or component I) and the electron-transfer Fe protein (also called dinitrogenase reductase or component II).^{34,38–41} (ii) A reducing source and MgATP are required for catalysis.^{42–45} (iii) Fe protein and MoFe protein associate and dissociate in a catalytic cycle involving single electron transfer and MgATP hydrolysis.³⁸ (iv) It was discovered that the MoFe protein contains two metal clusters: the iron–molybdenum cofactor (FeMo-co),^{30,46} which provides the active site for substrate binding and reduction, and P-cluster, involved in electron transfer from the Fe protein to FeMo-co.^{39,47–50} (v) Crystallographic structures were solved for both Fe⁵¹ and MoFe^{32,48,52–54} proteins. (vi) Also, the alternative V- and Fe-type nitrogenases, in which the Mo of FeMo-co is replaced by V or Fe, were discovered.¹⁸ Despite this accumulation of functional and structural information, the catalytic mechanism remained elusive.

The years since the Burgess and Lowe review¹⁷ have seen profound advances in understanding many aspects of nitrogenase structure and function. For example, the solutions of a number of high-resolution X-ray structures of the nitrogenase component proteins^{55–69} have provided insights into the nature of the active site FeMo-cofactor, most recently identifying the presence of an interstitial C atom,^{70–77} while structures of the two proteins in the complex^{78–81} have identified their binding

interface (Figures 1 and 2) and its alterations with the state of the bound nucleotide.⁶⁷ Likewise, great strides have been made

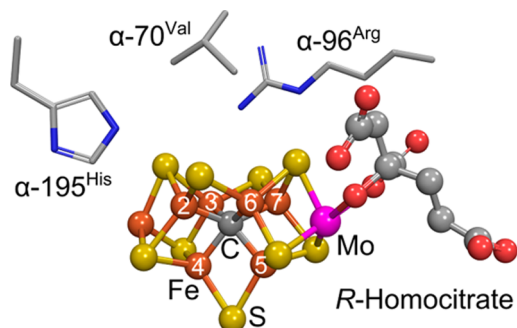


Figure 2. FeMo-cofactor and the side chains of selected amino acid residues of the MoFe protein. Numbering of iron atoms is according to the structure PDB coordinate 2AFK. Iron is shown in rust, molybdenum in magenta, nitrogen in blue, sulfur in yellow, carbon in gray, and oxygen in red.

in understanding the biosynthesis and insertion of the metal clusters of nitrogenase to form the mature proteins,^{21,82–89} and the properties of the V-type nitrogenase.^{90–98} Recent studies have begun to shed light on the order of events during the catalytic cycle,^{99–103} including the nature of electron transfer between the metal clusters^{62,104–111} and the roles of ATP binding and hydrolysis in these processes.^{55,68,99,112–121} Considerable progress has been made in the application of theoretical methods to various aspects of the nitrogenase mechanism.^{122–140} Finally, progress has been made in expanding in the substrates of nitrogenases^{93,141–149} to include CO^{95,96,98,150,151} and CO₂.^{148,152}

The present narrative focuses on recent progress in understanding the mechanism of N₂ activation and reduction to ammonia by Mo-nitrogenase. The discussion begins with a short reminder of the kinetic scheme that describes nitrogenase catalysis.^{33,103} It then turns to the successes in trapping catalytic intermediates of the MoFe protein by rapid freezing of turnover mixtures of Fe protein and of MoFe proteins, both wild-type and variants containing selected amino acid substitutions as a means to modulating reactivity.^{146,148,153,154} The use of EPR/ENDOR/ESEEM spectroscopic techniques applied to isotopically substituted trapped intermediates has allowed the identification and characterization of key intermediates along the N₂ reduction pathway.^{154–156} This led to the formulation of a reaction mechanism based on the properties of catalytic intermediates and grounded in the reaction of hydrides associated with FeMo-co.¹⁵⁶ The mechanism not only satisfies all constraints on the mechanism provided by earlier studies, but has suggested and passed a stringent test.¹⁵⁷ This report recounts these advances, and expands on them.

2. BACKGROUND

Two issues require consideration as a basis for discussion of recent advances in nitrogenase mechanism.^{155,156} The first is the kinetic model that has been developed to describe the multistep reduction of N₂ to two NH₃, and its implications for the stoichiometry of this reaction,^{33,103} implications that were mutually supported by experiment.¹⁵⁸ The second is the strategies and procedure that at last enabled the trapping of catalytic intermediates whose characterization by advanced

paramagnetic resonance techniques underlies the progress in mechanism described here.

2.1. Kinetics and Stoichiometry

A “kinetic” foundation for a nitrogenase mechanism was developed by extensive studies in the 1970s and 1980s by many groups, especially Lowe and Thorneley and their co-workers.^{17,33,103} The culmination of these extensive kinetic studies, which involved steady-state, stopped-flow, and freeze-quench kinetics measurements, was the Lowe–Thorneley (LT) kinetic model for nitrogenase function,^{17,33,103} which describes the kinetics of transformations among catalytic intermediates (denoted E_n) where n is the number of steps of electrons/protons delivery to MoFe protein, Figure 3. Electron transfer

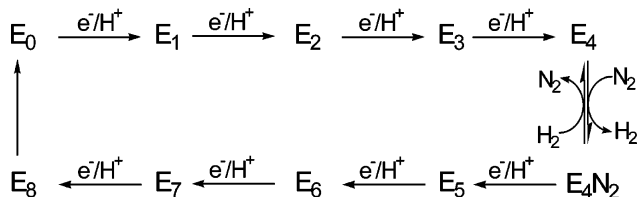
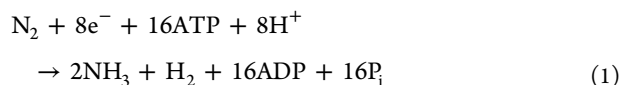


Figure 3. Simplified LT kinetic scheme that highlights correlated electron/proton delivery in eight steps. Although in the full LT scheme N₂ binds at either the E₃ or E₄ levels, the pathway through E₃ is de-emphasized here. LT also denotes the protons bound to FeMo-co (e.g., E₁H₁); for clarity we have omitted these protons in this scheme.

from Fe protein to MoFe protein is driven by the binding and hydrolysis of two MgATP species within the Fe protein;⁵⁹ the release of the Fe protein after delivery of its electron is the rate-limiting step of catalysis.³³

A central consequence of the kinetic measurements and defining feature of this scheme, Figure 3, is that the limiting enzymatic stoichiometry for enzyme-catalyzed nitrogen fixation is not what would be given by the simple balanced equation for reduction of N₂ to two NH₃ by six electrons/protons, but is given by eq 1



This is a conclusion that is in agreement with stoichiometric experiments by Simpson and Burris.¹⁵⁸ This equation highlights several key aspects of the nitrogenase mechanism, including the involvement of ATP hydrolysis in substrate reduction and the obligatory formation of 1 mol of H₂ per mole of N₂ reduced, an apparent “waste” of two reducing equivalents and four ATP per N₂ reduced.^{17,33}

Although the close of the previous millennium saw the accumulation of a vast breadth and depth of information about the reduction of N₂, H⁺, and a variety of other nonphysiological substrates,¹⁷ it was not until recently that studies have succeeded in characterizing E_n intermediate states beyond the resting-state E₀.^{154–156} Thus, the early studies provided little direct experimental evidence regarding a reaction pathway, and hence, there was no possibility of integrating a reaction pathway and kinetic scheme, as is central to development of a mechanism based on the properties of catalytic intermediates.¹⁵⁶

2.2. Trapping and Characterization of Substrates

The first 40 years of study of purified nitrogenase did not see the definitive characterization of any intermediates associated with the binding and reduction of N_2 ,¹⁵⁹ leaving the identity of the reaction pathway unresolved. The way forward was provided by studies of nitrogenases with individual amino acid substitutions, which revealed that the residue at position α -70 within the MoFe protein, a valine, acts as a “gatekeeper” that sterically controls the access of substrate to the active site FeMo-co (Figure 2).^{146,154} The side chain of this amino acid residue is located over one FeS face of FeMo-cofactor (that includes Fe atoms 2, 3, 6, and 7) thereby also implicating Fe as the site of substrate binding, while the α -195^{His} was inferred to be involved in proton delivery (Figure 2).^{160–165}

Use of MoFe protein substituted at one or both of these residues enabled freeze-quench trapping of a number of nitrogenase turnover intermediates, almost all of which show an EPR signal arising from an $S = \frac{1}{2}$ state of FeMo-co, rather than the $S = \frac{3}{2}$ state of resting-state FeMo-co.^{153,154} The procedures developed with these variants even enabled N_2 -intermediate trapping with enzyme.¹⁶⁶ The first fruit of this approach was the trapping of a state during reduction of the alkyne propargyl alcohol to the corresponding alkene.^{145,167} An intermediate trapped using MoFe protein variants was shown by ENDOR studies to be a wholly novel bio-organometallic structure in which the alkene product of alkyne reduction by nitrogenase binds as a π -complex/ferracycle to a single Fe ion of FeMo-cofactor, presumed to be Fe6.¹⁶⁸ This was followed by characterization of intermediates formed during the reduction of H^+ under Ar,¹⁶⁹ and, finally, identification of four associated with N_2 reduction itself.^{147,153,160,166,170,171}

Paramagnetic resonance methods have proven to be uniquely advantageous for characterization of trapped nitrogenase intermediates.¹⁵⁵ At the most basic level, FeMo-co in the E_0 resting-state of MoFe protein is an odd-electron (“Kramers”; half-integer spin, $S = \frac{3}{2}$)¹⁷², EPR-active cluster, and therefore, intermediate states that have accumulated an even number of electrons also will be EPR-active. Focusing on nitrogen fixation, FeMo-co then will be EPR-active in the E_n states, $n = 2, 4, 6, 8$, formed along the pathway for accumulation of the stoichiometrically required eight [e^-/H^+], eq 1. In contrast, E_n states $n = 1, 3, 5, 7$ will be even-electron, and FeMo-co will either be diamagnetic or in an integer-spin (“non-Kramers” spin-state)¹⁷³ cluster, which also can be EPR-active under appropriate conditions.^{173,174}

As will be illustrated below, electron-nuclear double-resonance (ENDOR) spectroscopy,^{175,176} supported by related techniques ESEEM and HYSCORE,¹⁷⁷ is uniquely suited for the study of freeze-quench trapped intermediates. These techniques give NMR-like spectra of nuclei that are hyperfine-coupled to the electron spin of an EPR-active cluster. The importance of the techniques rests on several aspects. ENDOR is *broad-banded*: with isotopic enrichment it can monitor *every* atom in a metalloenzyme active site. Thus, when interpreted in the context of the X-ray structure of the resting-state, it can reveal the electronic and metrical structure of a catalytic intermediate. It is *selective*: it interrogates only EPR-active states. It is *high-resolution*: it can resolve and interrogate the signals from multiple distinct EPR-active centers. It is *sensitive*: we have successfully analyzed the properties of intermediates present in ~20% abundance in a sample containing ~100 μM MoFe protein. Viewed another way, ENDOR is capable of

selecting and characterizing a small fraction of the MoFe protein in a sample. In contrast, for example, Mössbauer and X-ray absorption techniques, which have made enormous contributions to the study of resting-state nitrogenase, interrogate all FeMo-co in a sample, and if the state of interest is a small minority, its signal is buried and lost. Recently, however, an X-ray spectroscopic study has given information about a freeze-quenched nitrogenase intermediate.¹⁷⁸

3. INTERMEDIATES OF NITROGENASE ACTIVATION

According to the simplified LT kinetic scheme of Figure 3, the first four of the eight [e^-/H^+] of nitrogen fixation accumulate *prior* to N_2 binding, which occurs at the E_4 stage. The complete scheme^{17,33,103} allows for N_2 binding at E_3 as well, but E_4 uniquely places the enzyme on the pathway to N_2 hydrogenation.

3.1. E_1 – E_3

The E_1 state contains one-electron reduced cofactor, and has been assigned as an integer-spin species on the basis of Mössbauer studies of MoFe protein trapped during turnover under N_2 .^{179,180}

High-spin EPR signals ($S = \frac{3}{2}$), denoted as 1b and 1c, thought to be associated with E_n states, $n \leq 4$, were first observed 35 years ago for samples of wild-type nitrogenase trapped during turnover using a variety of conditions,¹⁸¹ and more recently were studied by rapid freeze-quench EPR.¹⁸² The kinetics of appearance of 1b and 1c demonstrated that they must be assigned to reduced states of cofactor, $n > 1$, rather than just as conformers of the FeMo-co resting-state. However, the kinetics of appearance of the stronger 1b signal was a puzzle: they were best described by assigning 1b to the E_3 state, which would seem to require that FeMo-co be in an integer-spin (non-Kramers) state, contrary to observation. Most likely, this apparent contradiction reflects uncertainties in the rate constants used in the kinetics analysis, and 1b represents an E_2 state. During cryoannealing experiments¹⁸³ discussed below, we definitively observed that FeMo-co of E_2 is in a high-spin ($S = \frac{3}{2}$) state, but at least in the α -70^{Ile} variant its g-values were distinct from those of 1b. The spectrum of the 1c species is weaker in intensity. It may represent a conformer of the resting or 1b states, or may correspond to even more reduced states, as its effective formation requires a high molar ratio of Fe protein to MoFe protein, corresponding to higher electron flux.

3.2. E_4 : The “Janus Intermediate”

In this subsection we describe the trapping and EPR/ENDOR characterization of the E_4 intermediate as activated by the accumulation of four [e^-/H^+] for binding and reduction of N_2 . The structure of E_4 as determined by ENDOR spectroscopy, and integrated into the LT kinetic scheme, has been the key to recognizing the central role of hydrides in the mechanism for nitrogen fixation.¹⁵⁶ We then discuss the E_1 – E_4 states associated with electron accumulation by MoFe protein; subsequent sections discuss the trapped states associated with the N_2 reduction pathway following N_2 binding.

Early in the search for intermediates,¹⁴⁶ the α -70^{Val → Ile} substitution in the MoFe protein was shown to deny access of all substrates to the active site, except protons.^{169,184} Samples of this substituted MoFe protein freeze-quenched during turnover under Ar exhibited a new $S = \frac{1}{2}$ EPR signal,¹⁶⁹ which also can be observed at lower concentrations during turnover of wild-type MoFe protein under Ar.^{181,185} ^{1,2}H ENDOR spectroscopic analysis of this trapped state¹⁶⁹ revealed the

presence of two strongly hyperfine-coupled, metal-bridging hydrides [$M-H-M'$]: (i) The finding that the bound hydrides have a large isotropic hyperfine coupling, $a_{iso} \approx 24$ MHz, led to their assignment as hydrides bound to metal ion(s) of the core. (ii) The anisotropic hyperfine contribution, $T = [-13.3, 0.7, 12.7]$ MHz, exhibits almost complete rhombicity, as defined by the form $T_{rh} \approx [t, 0, -t]$. This form rules out terminal hydrides, which would have a roughly axial T^{186} and is precisely the form first predicted¹⁸⁷ and then confirmed¹⁸⁸ to be associated with a hydride bridging two paramagnetic metal ions, namely as $[Fe-H-Fe]$ and/or $[Mo-H-Fe]$ fragments.

^{95}Mo ENDOR measurements subsequently established that both hydrides bridge two Fe ions, forming two $[Fe-H-Fe]$ fragments (Figure 4), as follows.¹⁸⁹ Equations for the

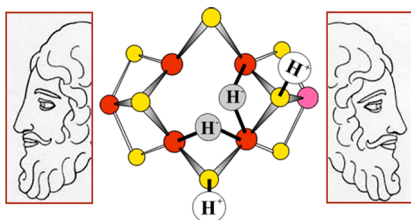
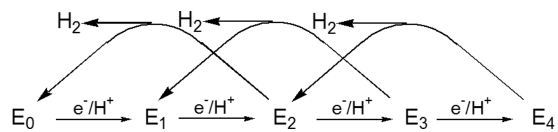


Figure 4. Depiction of E_4 as containing two $[Fe-H-Fe]$ moieties, emphasizing the essential role of this key “Janus intermediate”, which comes at the halfway point in the LT scheme, having accumulated four $[e^-/H^+]$, and whose properties have implications for the first and second halves of the scheme. Janus image adapted from http://www.plotinus.com/janus_copy2.htm. Figure adapted with permission from ref 156. Copyright 2013 American Chemical Society.

anisotropic hyperfine interaction matrix, T , of a nucleus that undergoes through-space dipolar interactions to two spin-coupled metal ions¹⁸⁷ were generalized to describe an arbitrary $[M_1-H-M_2]$ fragment of a spin-coupled cluster. The components of T are a function of the $[M_1-H-M_2]$ geometry and of the coefficients $[K_1, K_2]$ that describe the projection of the total cluster spin on the two local M-ion spins. The ^{95}Mo ENDOR measurements of the intermediate showed a very small isotropic hyperfine coupling, $a_{iso}(^{95}Mo) \sim 4$ MHz, which indicated that K_{Mo} is too small to yield the rhombic dipolar coupling, T_{rh} , observed in this intermediate.¹⁸⁹ The model for E_4 displayed in Figure 4 is completed by placement on sulfurs of the two protons^{190,191} that form part of the delivery of $4[e^-/H^+]$ (Figure 3). The protons are so placed because they must be near to the negative charge density associated with the hydrides in order to obtain the electrostatic stabilization implicit in the required accumulation of one proton for each electron delivered to MoFe protein;¹⁷ other arrangements are possible, such as putting both protons on doubly bridging sulfur, but see below.

Cryoannealing this “dihydride” intermediate in the frozen state at -20 °C, which prevents further delivery of electrons from the Fe protein, showed that it relaxes to the resting FeMo-co state by the successive loss of two H_2 molecules.¹⁸³ According to the LT scheme, only E_4 would undergo this two-step relaxation process (Scheme 1), with the first relaxation step of E_4 yielding H_2 and the E_2 state, the second step returning FeMo-co to the E_0 stage with loss of a second H_2 , and the production of H_2 being revealed by solvent kinetic isotope effects in both stages. This relaxation protocol thus revealed that the trapped intermediate is the E_4 state, which has accumulated $n = 4$ electrons and protons.¹⁸³ As the relaxation

Scheme 1



measurements involved tracking the kinetically linked conversion of E_4 into E_2 , and the conversion of E_2 into resting-state E_0 , the measurements further allowed an unambiguous identification of the EPR signal associated with E_2 (see above).

Examination of the simplified version of the LT scheme of Figure 3 reveals that E_4 is a key stage in the process of N_2 reduction.^{33,103} Indeed, we have denoted it as the “Janus” intermediate, referring to the Roman God of transitions who is represented with two faces, one looking to the past and one looking to the future (Figure 4).¹⁵⁶ Looking “back” from E_4 to the steps by which it is formed, E_4 is the culmination of one-half of the electron/proton deliveries during N_2 fixation: four of the eight reducing equivalents are accumulated in E_4 , before N_2 even becomes involved. Looking “forward”, toward NH_3 formation, E_4 is the state at which N_2 hydrogenation begins, and it is involved in one of the biggest puzzles in N_2 fixation: “why” and “how” H_2 is lost upon N_2 binding.

To date, we have visualized E_4 by placing its two hydrides on the Fe2, 3, 6, 7 face of resting-state FeMo-co and sharing a common vertex at Fe6, Figure 4. Although the hydrides may well exhibit fluxionality at ambient temperature, their ability to adopt a configuration with a common vertex is required by the *reductive elimination* (re) mechanism of reversible H_2 release upon N_2 binding (section 7), and Fe6 is favored from earlier kinetic studies on MoFe protein variants.^{69,144,145,154,166,168} However, this model is only one of four possible configurations based on the resting structure that have two hydrides sharing an Fe6 vertex. To visualize these structures we have built the bound hydrides onto the crystal structure of resting-state FeMo-co using Fe–H distances from model complexes,^{188,192} Figure 5.

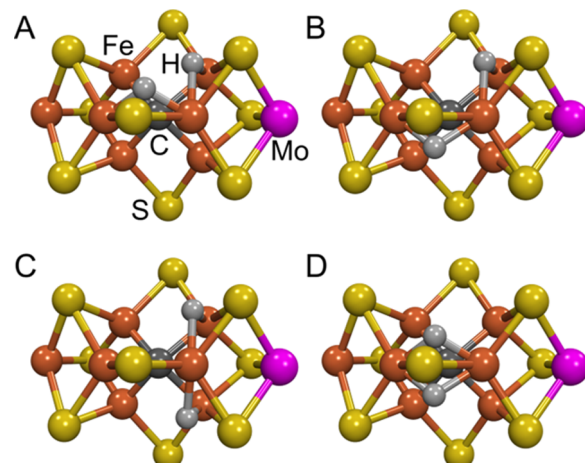


Figure 5. Mockups of the “Janus” E_4 intermediate in which the two bridging hydrides $[Fe-H-Fe]$ revealed by ENDOR spectroscopy are built onto the resting-state crystal structure. These models of FeMo-co have Fe6 as a “vertex” for the two bridging hydrides to facilitate reductive elimination. The figure was generated using the coordinate file PDB:2AFK. Iron is shown in rust, molybdenum in magenta, sulfur in yellow, carbon in dark gray, and hydrogen in light gray.

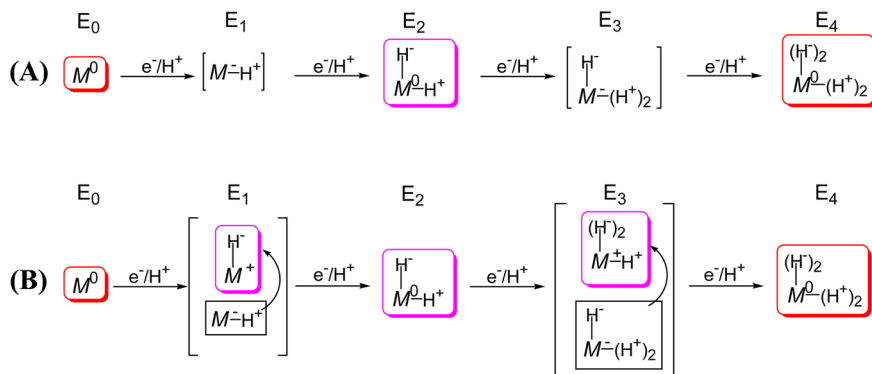


Figure 6. Formulations of E_1 – E_4 derived from consideration of E_4 as containing two bound hydrides and two protons. (A) Assuming reduction of the core in $n = 1, 3$ states. (B) Alternative formulation of E_1 – E_4 under the assumption of hydride formation at every stage, in which case the core is formally oxidized for E_n , $n = 1, 3$. Symbols: M represents FeMo-co core; superscripts are charge difference between core and that of resting-state (commonly denoted M^N); the number of bound protons/hydrides are indicated. Adapted with permission from ref 156. Copyright 2013 American Chemical Society.

Quantum chemical computations will test these alternatives. However, the experimentally determined relative orientation of the hyperfine tensors of the two hydrides provides a significant constraint on their placement within E_4 . Given the stability of the FeMo-co structure that is likely imparted by the interstitial carbide, it seemed plausible to us that consideration of the constructed models of Figure 5 would allow us to test these alternative hydride distributions, even though it is beyond doubt that the structure of FeMo-co will distort upon substrate binding. This exercise (see Supporting Information) provides support for the *topology* of hydride binding pictured for the Janus E_4 intermediate in Figure 4, with hydrides bridging Fe2/Fe6 and Fe6/Fe7 (Figure 5A,B), as opposed to Figure 5C,D, but does not discriminate between the structures of Figure 5A,B. In discussions below, we retain the placement of the E_4 hydrides shown in Figure 4 (Figure 5A) as being more readily visualized in discussions of mechanism.

The characterization of the hyperfine interactions of the metal-ion core of E_4 that began with the ^{95}Mo ENDOR measurements¹⁸⁹ was completed by an ENDOR study of the ^{57}Fe atoms of the E_4 FeMo-co through use of a suite of advanced ENDOR methods.¹⁹³ The determination of hyperfine interactions for two ligand hydrides and all eight metal ions of FeMo-cofactor in this state will provide the experimental test that guides future computational studies that seek to characterize the geometric and electronic structure of E_4 .

Storage of the reducing equivalents accumulated in the E_4 state as bridging hydrides has major consequences. A bridging hydride is less susceptible to protonation than a terminal hydride, and thus bridging hydride(s) diminish the tendency to lose reducing equivalents through the formation of H_2 (Scheme 1), thereby facilitating the accumulation of reducing equivalents by FeMo-co. This mode also lowers the ability of the hydrides to undergo exchange with protons in the environment, a characteristic that is shown to be of central importance below. However, the bridging mode also lowers hydride reactivity toward substrate hydrogenation, relative to that of terminal hydrides.^{194,195} As a result, substrate hydrogenation most probably incorporates the conversion of hydrides from bridging to terminal binding modes.¹⁹⁶ We next discuss how the structure found for E_4 guides assignment of structures for the E_1 – E_3 states. Subsequently, we show how the E_4 structure defined possible mechanisms for coupling H_2 loss to N_2 binding.

3.3. Redox Behavior and Hydride Chemistry of E_1 – E_3 : Why Such a Big Catalytic Cluster?

Given that the four accumulated electrons of E_4 reside not on the metal ions but, instead, are formally assigned to the hydrides of the two Fe-bridging hydrides, what then are the proper descriptions of E_1 – E_3 ? The addition of one electron/proton to the MoFe protein results in the E_1 state, and a Mössbauer study of nitrogenase trapped during turnover under N_2^{180} suggested that this state contains the reduced metal-ion core of FeMo-co, denoted M^- in Figure 6A. The presence in E_4 of two bridging hydrides/two protons led us to propose that upon delivery of the second electron/proton to form E_2 the metal–sulfur core of the FeMo-cofactor “shuttles” both electrons onto one proton to form an $[\text{Fe}–\text{H}–\text{Fe}]$ hydride, leaving the second proton bound to sulfur for electrostatic stabilization and the core formally at the resting-state, M^0 , redox level (also commonly referred to as, M^N),¹⁹⁷ Figure 6A. A subsequent, analogous, two-stage process would then yield the E_4 state, with its two $[\text{Fe}–\text{H}–\text{Fe}]$ hydrides, two sulfur-bound protons, and the core at the resting-state, M^0 , redox level.¹⁹³

Such a process of acquiring the four reducing equivalents of E_4 involves only a single redox couple connecting two formal redox levels of the FeMo-co *core* of eight metal ions; M^0 the resting-state, and M^- the one-electron reduced state of the core, Figure 6A.¹⁹³ Indeed, comparisons of the ^{57}Fe ENDOR results for the E_4 intermediate with earlier ^{57}Fe ENDOR studies and “electron inventory analyses”^{155,198} of nitrogenase intermediates led us to the remarkable suggestion that, throughout the nitrogenase catalytic cycle, the FeMo-cofactor would cycle through only two formal redox levels of the metal-ion core. On reflection, it seems obvious that only by “storing” the equivalents as hydrides is it possible to accumulate so much reducing power at the constant potential of the Fe protein. We further proposed that such “simple” redox behavior of a complex metal center might apply to other FeS enzymes carrying out multielectron substrate reductions.¹⁹³

Considering the critical role of hydrides in storing reducing equivalents, we also suggested that the E_1 and E_3 states, respectively, might well contain one and two bridging hydrides bound to a formally *oxidized* metal-ion core (Figure 6B),¹⁰⁰ in which case the single redox couple accessed would formally be that between M^0 and M^+ . In section 9, below we adopt this “oxidative” formulation of the E_1 – E_3 structures. We emphasize

that a third formulation of $E_1(E_3)$, with hydride(s) bound to M⁰ and the presence of oxidized P-cluster, is ruled out by the absence of EPR signals from P⁺ in samples trapped under turnover conditions.

If the FeMo-cofactor does not utilize more than one redox couple during catalysis, then why is it constructed from so many metal ions? As discussed above, the hydrides of E₄ bind to at least two, and plausibly three Fe atoms of a 4-Fe face of FeMo-co, as shown in Figures 4 and 5. It is further possible that catalysis is modulated by the linkage of Fe ion(s) to the anionic atom C that is centrally located within the metal–sulfur core of the FeMo-cofactor.^{70,71} Formation of such a 4Fe face and the incorporation of C is not likely with less than a trigonal prism of six Fe ions linked by sulfides to generate these structural features. In this view, the trigonal prismatic FeMo-cofactor core of six Fe ions plus C generates the catalytically active 4Fe face. This prism is capped, and its properties are likely “tuned”, by two “anchor” ions, one Fe plus a Mo, or a V or Fe in the alternative nitrogenases.

Finally, and far from least, as we have consistently noted (see section 7), there is good reason to imagine N₂ and/or the N₂H_x reduction intermediates may interact with multiple Fe ions on a FeMo-co face.

3.4. Why Does Nitrogenase Not React with H₂/D₂/T₂ in the Absence of N₂?

The following question is commonly raised: If electrons accumulated in E_n intermediates, $n = 2–4$, can relax to E_{n-2} through formation and release of H₂ during turnover, as captured in the partial LT scheme, Scheme 1, why does the enzyme not exhibit the reverse of this reaction, and react with H₂/D₂ in what might appear to be the “microscopic reverse” of H₂ release? We have proposed that H₂ formation involves protonation of an [Fe–H–Fe], and at a basic level, all three relaxation processes of Scheme 1 should have much the same characteristics. For simplicity in addressing this issue, we focus on the “first” of these, the $E_2 \rightarrow E_0$ relaxation, and ask why E_0 is not reduced by H₂ to form E_2 , eq 2



A logical answer to this question begins with the recognition that the LT kinetic scheme for N₂ fixation, Figure 3 (also denoted the “MoFe protein cycle”), and the segment presented in Scheme 1, omit the reactions of the Fe protein for clarity; these are treated as a separate “Fe-protein cycle”.^{17,33,103,154} A stoichiometrically correct scheme that merges the Fe protein and MoFe protein cycles is given in Figure 7. It reminds us that E_2 is formed by two steps of Fe → MoFe protein ET, with each step involving hydrolysis of two ATP molecules to drive a reaction that is highly “uphill” energetically.

Clearly the $E_2 \rightarrow E_0$ relaxation with accompanying loss of H₂ is *not* the “reverse” of the turnover formation of E_2 from E_0 ; neither Fe protein reduction nor ATP formation is involved. Instead, it is a side-reaction of E_2 . Indeed, it is even quite unlikely that a direct reaction of H₂ with E_0 to form E_2 (eq 2) would be the microscopic reverse of the $E_2 \rightarrow E_0$ relaxation with accompanying loss of H₂. Moreover, the steric congestion caused by the sulfurs at the six tetrahedral [FeS₃C] sites of the FeMo-co “waist” requires that the core must relax for the Fe to bind any ligand; in particular it is probable that the structure of the [Fe₇S₉MoC] core of FeMo-cofactor of E_0 (denoted M^N) is altered during the reduction of E_0 by two [e⁻/H⁺] to form E_2 (also see section 9.2). In this case, as illustrated in Figure 7, the

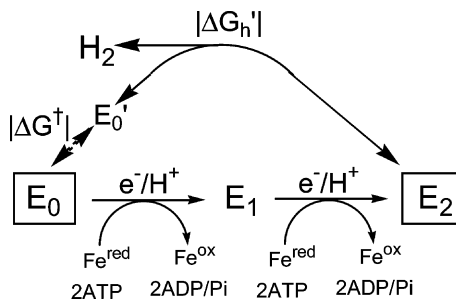


Figure 7. Formation and relaxation of E_2 . In-line: The “on-path” two-step, ATP-dependent addition of two H^+/e^- to MoFe protein to form E_2 . Off-line: Representation of the exergonic (free energy, $+|\Delta G_h'|$) “off-path” relaxation of E_2 , liberating H₂ and directly regenerating E_0 without intervention of Fe protein, and of the energetically (free energy, $+|\Delta G_h'|$) and kinetically forbidden reverse of this process; E_0' is a putative intermediate state that causes the reaction of E_0 not to be the microscopic reverse of the release of H₂ from E_2 (see text).

relaxation of E_2 with loss of H₂ to form the resting E_0 state would be a 2-step process. The loss of H₂ by E_2 would be expected to form a state (denoted here E_0') that contains FeMo-cofactor in a conformation approximating that of E_2 , corresponding to a metastable conformation of its resting redox level (denoted M^{N'}); this conformer would in turn undergo a $M^{N'} \rightarrow M^N$ structural relaxation associated with $E_0' \rightarrow E_0$ relaxation. The reduction of E_0 by H₂ (eq 2) by the microscopic reverse of this two-step relaxation would correspondingly take place in two steps, Figure 7, with the initial $E_0 \rightarrow E_0'$ thermal activation associated with the conformational change, $M^N \rightarrow M^{N'}$, adding an activation free energy (denoted $|\Delta G^\ddagger|$) and kinetic barrier to the endergonic reduction of $E_0' \rightarrow E_2$ by H₂ (free energy denoted $|\Delta G_h'|$).

What would be the free energy for reduction of nitrogenase by H₂, as in eq 2? An upper bound for the free energy change for this reaction, ΔG_{h2} , would be 4 times the negative of the free energy change for the hydrolysis of ATP to form ADP and P_i ($-\Delta G_{\text{Hyd}} \sim +7 \text{ kcal/mol}$; total, endergonic by $\sim +28 \text{ kcal/mol}$), that is required for the formation of E_2 through the delivery of reducing equivalents by Fe protein; roughly compatible with that, oxidative addition of H₂ to an Fe–S center (hydrogenase), corresponding to $|\Delta G_h'|$, is uphill by at least $+20 \text{ kcal/mol}$,^{199,200} to which must be added the conformational free energy $|\Delta G^\ddagger|$. Given the strongly endergonic nature of eq 2, coupled with the kinetic penalty associated with the activation of E_0 to E_0' , it becomes clear why H₂ is not observed to reduce FeMo-cofactor.

4. “DUELING” N₂ REDUCTION PATHWAYS

Researchers have long considered two competing proposals for the second half of the LT kinetic scheme, the reaction pathway for N₂ reduction that begins with the Janus E₄ state.^{17,139,155} These invoke distinctly different intermediates, Figure 8, and computations suggest they likely involve different metal-ion sites on FeMo-co.¹³⁹ The “distal” (D) pathway is associated with the Chatt^{4,201} or Chatt–Schrock cycle³ because it is utilized by inorganic Mo complexes discovered by these investigators to cleave N₂ (Chatt and co-workers^{202,203}) and, most dramatically, to catalytically fix N₂ (Schrock and co-workers^{24,204–206}). In this cycle, which has been suggested to apply to nitrogen fixation by nitrogenase with Mo as the active site,¹³⁹ a single N of N₂ is hydrogenated in three steps until the first NH₃ is liberated, and then the remaining nitrido-N is

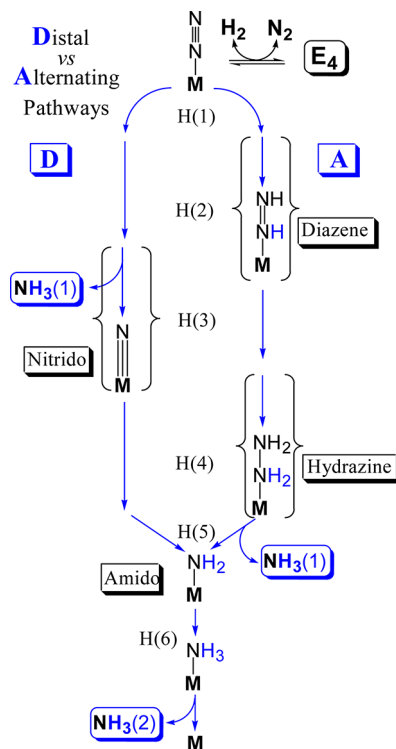


Figure 8. Comparison of distal (D) and alternating (A) pathways for N_2 hydrogenation, highlighting the stages that best distinguish them, most especially noting the different stages at which $\text{NH}_3(1)$ is released.

hydrogenated three more times to yield the second NH_3 . In the “alternating” (A) pathway that has been suggested to apply to catalysis at Fe of FeMo-co,^{25,131} the first two hydrogenations generate a diazene-level intermediate, the next two form hydrazine, and the first NH_3 is liberated only by the fifth hydrogenation (Figure 8). As one can imagine alternative structures for the intermediates, the figure focuses on the defining difference between D and A pathways as being the release of the first NH_3 in the D as occurring after three hydrogenations of substrate, the addition of three $[\text{e}^-/\text{H}^+]$ to substrate, but only after five hydrogenations in A.

Simple arguments can be made for both pathways and for either Fe and Mo as the active site.^{17,154,155,207} For example, the A route is suggested by the fact that hydrazine is both a substrate of nitrogenase and is released upon acid or base hydrolysis of the enzyme under turnover,^{17,208–211} and is favored in computations with reaction at Fe,¹³¹ while the D route was suggested by the fact that until recently the only inorganic complexes that catalytically fix N_2 employ Mo and function via the D route,²⁴ which is computationally favored for reaction at Mo.¹³⁹ Interestingly, this argument is somewhat weakened by a recent study that reported small W clusters fix N_2 by the A pathway.²¹² More significantly, the argument based on N_2 cleavage and catalytic N_2 fixation by Mo model complexes has lost ground by the quite recent discovery of Fe model complexes that cleave N_2 (Holland and co-workers^{22,213}) and indeed that also catalytically fix N_2 (Peters and co-workers²¹⁴).

Further support for the A pathway is provided by considerations of the alternative nitrogenases. It is most economical to suggest that both the Mo-dependent nitrogenase studied here and the V-type nitrogenase reduce N_2 by the same pathway. As V-nitrogenase produces traces of N_2H_4 while

reducing N_2 to NH_3 ,²¹⁵ then according to Figure 8 this enzyme can be concluded to function via the A pathway, implying the same is true for Mo-nitrogenase.

5. INTERMEDIATES OF N_2 REDUCTION: E_N , $N \geq 4$

As can be seen in Figure 8, characterization of catalytic intermediates formed during the reduction of N_2 could distinguish between the D and A pathways. However, such intermediates had long eluded capture until four intermediates associated with N_2 fixation were freeze-trapped and characterized by ENDOR spectroscopic studies.^{154,155} These four states were generated under the hypothesis that intermediates associated with different reduction stages could be trapped using N_2 or semireduced forms of N_2 or their analogues: N_2 ; $\text{NH}=\text{NH}$; $\text{NH}=\text{N}-\text{CH}_3$; $\text{H}_2\text{N}-\text{NH}_2$.^{17,153,154} These included a proposed early (e) stage of the reduction of N_2 , $\text{e}(\text{N}_2)$, obtained from wild-type (WT) MoFe protein with N_2 as substrate;^{166,170} two putative “midstage” intermediates, $m(\text{NH}=\text{N}-\text{CH}_3)$, obtained from α -195^{Gln} MoFe protein with $\text{CH}_3-\text{N}=\text{NH}$ as substrate^{170,171} and $m(\text{NH}=\text{NH})$, obtained from the doubly substituted, α -70^{Ala}/ α -195^{Gln} MoFe protein during turnover with *in-situ*-generated $\text{NH}=\text{NH}$;¹⁴⁷ and a “late” stage, $\text{l}(\text{N}_2\text{H}_4)$, from the α -70^{Ala}/ α -195^{Gln} MoFe protein during turnover with $\text{H}_2\text{N}-\text{NH}_2$ ^{160,170} as substrate. Both hydrazine and diazene are substrates of wild-type nitrogenase that, like N_2 , are reduced to ammonia.^{17,147,160,211,216}

5.1. Intermediate I

A combination of X/Q-band EPR and $^{15}\text{N},^{1}\text{H}$ ENDOR measurements on the intermediates formed with the three semireduced substrates during turnover of the α -70^{Val \rightarrow Ala}/ α -195^{His \rightarrow Gln} MoFe protein subsequently showed that in fact they all correspond to a common intermediate (here denoted I) in which FeMo-co binds a substrate-derived $[\text{N}_x\text{H}_y]$ moiety (Figure 9).^{154–156,207} Thus, both the diazenes and hydrazine enter and “flow through” the normal N_2 -reduction pathway (Figure 8), and the diazene reduction must have “caught up” with the “later” hydrazine reaction.

^{1}H and ^{15}N 35 GHz CW and pulsed ENDOR measurements next showed that I exists in two conformers, each with metal ion(s) in FeMo-co having bound a single nitrogen from a substrate-derived $[\text{N}_x\text{H}_y]$ fragment.^{154,155} Subsequent high-resolution 35 GHz pulsed ENDOR spectra and X-band HYSCORE measurements showed no response from a second nitrogen atom, and when I was trapped during turnover with the selectively labeled $\text{CH}_3-\text{N}=\text{NH}$, $^{13}\text{CH}_3-\text{N}=\text{NH}$, or $\text{C}^2\text{H}_3-\text{N}=\text{NH}$, no signal was seen from the isotopic labels.²⁰⁷ From these results we concluded the N–N bond had been cleaved in forming I, which thus represents a late stage of nitrogen fixation, after the first ammonia molecule already has been released and only a $[\text{NH}_x]$ ($x = 2$ or 3) fragment of substrate is bound to FeMo-co.²⁰⁷

5.2. Nitrogenase Reaction Pathway: D versus A

Given that states that could correspond to I are reached by both A and D pathways (Figure 8), the identity of this $[\text{NH}_x]$ moiety need not in itself distinguish between pathways. However, the spectroscopic findings about I, in conjunction with a variety of additional considerations, led us to propose that nitrogenase functions via the A reaction pathway of Figure 8 for reduction of N_2 .²⁰⁷ As one example, to explain how nitrogenase could reduce each of the substrates, N_2 , N_2H_2 , and N_2H_4 , to two NH_3 molecules via a common A reaction pathway, one need only postulate that each substrate “joins” the

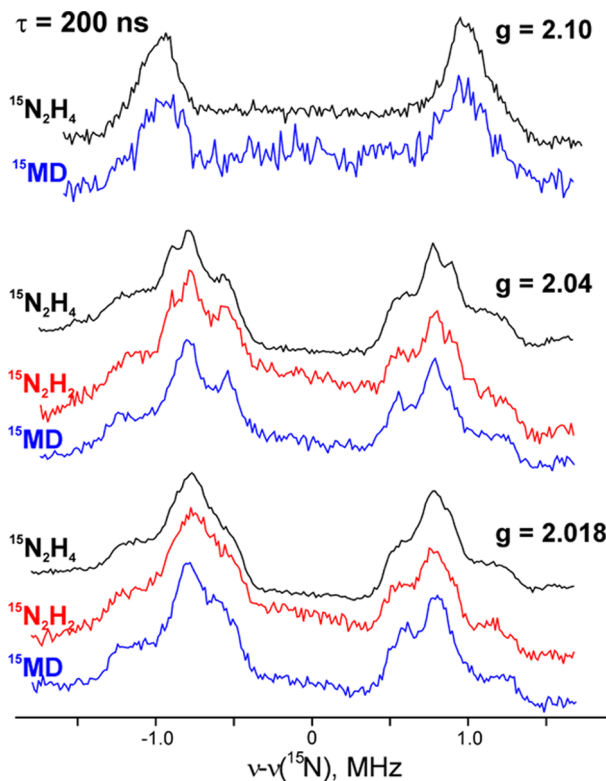


Figure 9. Comparison of 35 GHz ReMims pulsed ^{15}N ENDOR spectra of intermediates trapped during turnover of the α -70^{Val}-Ala/ α -195^{Gln} MoFe protein with $^{15}\text{N}_2\text{H}_4$, $^{15}\text{N}_2\text{H}_2$, and $^{15}\text{NH}=^{14}\text{N}-\text{CH}_3$ (denoted ^{15}MD). Adapted with permission from ref 207. Copyright 2011 American Chemical Society.

pathway at the appropriate stage of reduction, binding to FeMo-co that has been “activated” by accumulation of a sufficient number of electrons (possibly with FeMo-co reorganization), and then proceeds along that pathway. Energetic considerations,¹³⁹ in combination with the strong influence of α -70^{Val} substitutions of MoFe protein without modification of FeMo-co reactivity, then implicate Fe, rather than Mo, as the site of binding and reactivity.^{146,154,217}

5.3. Intermediate H

When nitrogenase is freeze-quenched during turnover, the EPR signals from trapped intermediates in odd-electron FeMo-co states (Kramers states; $S = 1/2, 3/2, \dots$; $E_n, n = \text{even}$),^{154,155} plus the signals from residual resting-state FeMo-co, never quantitate to the total FeMo-co present, indicating that EPR-silent states of FeMo-co must also exist. These silent MoFe protein states must contain FeMo-co with an even number of electrons, and thus correspond to $E_n, n = \text{odd}$ ($n = 2m+1, m = 0-3$) intermediates in the LT scheme. As noted above, such states may contain diamagnetic FeMo-co, or FeMo-co in integer-spin ($S = 1, 2, \dots$), “non-Kramers (NK)” states,^{179,180,218} but no EPR signal from an integer-spin form of FeMo-co had been detected until careful examination of samples that contain intermediate I¹⁵⁴⁻¹⁵⁶ revealed an additional broad EPR signal at low field in Q-band spectra that arises from an integer-spin system with a ground-state non-Kramers doublet with spin $S \geq 2$ (Figure 10).²¹⁹

Earlier work showed how to characterize a non-Kramers doublet with ESEEM spectroscopy (NK-ESEEM),^{173,174} so NK-ESEEM time-waves were collected for the NK intermediates trapped during turnover with: ^{14}N and ^{15}N

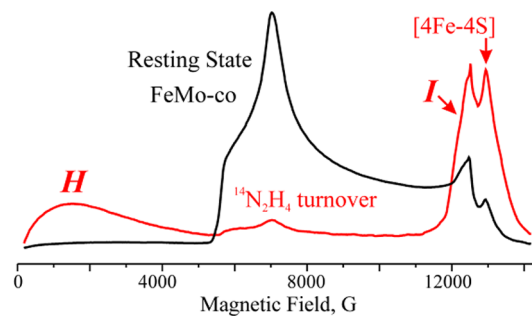


Figure 10. 2K Q-band CW EPR spectrum of α -70^{Val}-Ala, α -195^{His}-Gln MoFe protein in resting-state ($S = 3/2$) and trapped during turnover with $^{14}\text{N}_2\text{H}_4$. Kramers intermediate I and non-Kramers intermediate, H, are noted in the turnover spectrum. Adapted with permission from ref 219. Copyright 2012 National Academy of Sciences.

isotopologs of N_2H_2 and N_2H_4 substrates; ^{95}Mo -enriched α -70^{Val}-Ala/ α -195^{His}-Gln MoFe protein; H— $^{14}\text{N}=^{14}\text{N}-\text{CH}_3$, H— $^{15}\text{N}=^{14}\text{N}-\text{CH}_3$, and H— $^{14}\text{N}=^{14}\text{N}-\text{CD}_3$. Figure 11

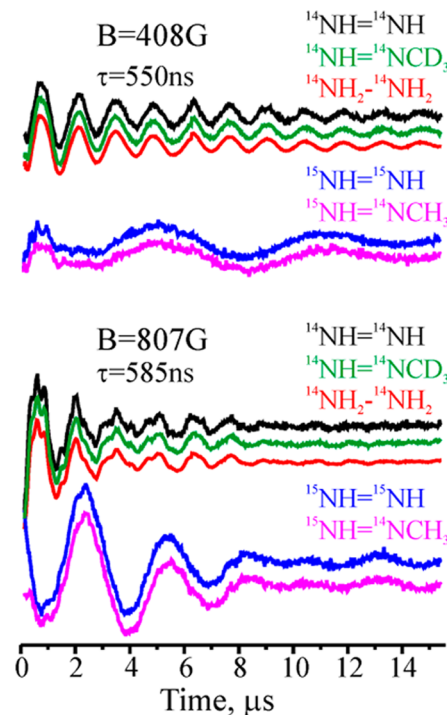


Figure 11. Three-pulse ESEEM traces after decay-baseline subtraction for NK intermediate H of α -70^{Val}-Ala, α -195^{His}-Gln MoFe protein trapped during turnover with $^{14}\text{NH}=^{14}\text{NH}$, $^{14}\text{NH}=^{14}\text{NCD}_3$, $^{14}\text{NH}_2-^{14}\text{NH}_2$, $^{15}\text{NH}=^{15}\text{NH}$, $^{15}\text{NH}=^{14}\text{NCH}_3$. Adapted with permission from ref 219. Copyright 2012 National Academy of Sciences.

presents representative 35 GHz (2 K) three-pulse NK-ESEEM time-waves collected at several relatively low fields from the nitrogenase NK intermediates generated with isotopologues of the three substrates. The NK-ESEEM time-waves for the intermediates trapped during turnover with the corresponding ^{14}N and ^{15}N isotopologues of N_2H_2 , N_2H_4 , and HN_2CH_3 substrates are identical at all fields, indicating that they are associated with a common intermediate, denoted H, trapped during turnover with all three substrates. ^{95}Mo enrichment of α -70^{Val}-Ala, α -195^{His}-Gln MoFe protein produces a significant

change of the NK-ESEEM time-wave. This analysis established that the NK-EPR signal of **H** arises from the Mo-containing FeMo-co in an integer-spin-state with $S \geq 2$, and not the all-iron electron-transfer P cluster, also present in the MoFe protein, or even the [4Fe–4S] cluster of the Fe protein.²¹⁹

Comparison of the $^{14}\text{N}/^{15}\text{N}$ NK-ESEEM of **H** in Figure 11 indicates that a nitrogenous ligand derived from substrate is directly bound to FeMo-co of $\alpha\text{-}70^{\text{Val} \rightarrow \text{Ala}}/\alpha\text{-}195^{\text{His} \rightarrow \text{Gln}}$ MoFe protein. Modulation is absent from the second ^{14}N that would be present if the N–N bond of substrate remained intact, as shown by comparison of the time-waves for the **H** prepared with $\text{H}-^{15}\text{N}=\text{NH}_2-\text{H}$ versus $\text{H}-^{15}\text{N}=\text{NH}_2-\text{CH}_3$, as is modulation from ^2H of $\text{H}-^{14}\text{N}=\text{NH}_2-\text{CD}_3$. This indicates that **H** contains an NH_x fragment that remains bound to FeMo-co after cleavage of the N–N bond and loss of NH_3 . Quadrupole coupling parameters for the NH_x fragment indicated it is not NH_3 , and that **H** has bound $[-\text{NH}_2]$.²¹⁹

6. UNIFICATION OF THE NITROGENASE REACTION PATHWAY WITH THE LT KINETIC SCHEME

The **H** and **I** intermediates provide “anchor-points” that allow assignment of the complete set of E_n intermediates that follow E_4 , $5 \leq n \leq 8$. As illustrated in Figure 12, the loss of two

reducing equivalents and two protons as H_2 (eq 1) upon N_2 binding to the FeMo-co of E_4 leaves FeMo-co activated by two reducing equivalents and two protons. We argued that when N_2 binds to FeMo-co it is “nailed down” by prompt hydrogenation, Figure 12, with N_2 binding, H_2 loss, and reduction to the diazene level, all occurring at the E_4 kinetic stage of the LT scheme.²¹⁹ The identification of **H** with its E_n stage is achieved as follows. (i) As the same intermediate **H** is formed during turnover with the two diazenes and with hydrazine, the diazenes must have catalytically “caught up” to hydrazine, and **H** must occur at or after the appearance of a hydrazine-bound intermediate. (ii) As noted above, **H** contains FeMo-co in an integer-spin (NK) state, and thus corresponds to an E_n state with $n = \text{odd}$. As **H** is a common intermediate that contains a bound fragment of substrate, it must, therefore, correspond to E_5 or E_7 , and analysis of the pathway alternatives in the light of the EPR/ESEEM measurements indicated that **H** corresponds to the $[\text{NH}_2]^-$ -bound intermediate formed subsequent to N–N bond cleavage and NH_3 release at the E_7 stage of the P–A pathway.

By parallel arguments, the only possible assignment for the $S = 1/2$ state **I**, which we showed earlier to occur after N–N bond cleavage,²⁰⁷ is as E_8 : **I** must correspond to the final state in the catalytic process (Figure 12), in which the NH_3 product is bound to FeMo-co at its resting redox state, prior to release and regeneration of the resting-state form of the cofactor. The trapping of a product-bound intermediate **I** is analogous to the trapping of a bio-organometallic intermediate during turnover of the $\alpha\text{-}70^{\text{Val} \rightarrow \text{Ala}}$ MoFe protein with the alkyne, propargyl alcohol; this intermediate was shown to be the allyl alcohol alkene product of reduction.¹⁶⁸ With assignments of E_4 , E_7 , and E_8 , then filling in the LT “boxes” for E_5 , E_6 of Figure 3 is straightforward, thus unifying the reaction pathway for N_2 reduction with the LT scheme.

Figure 12 adopts a “prompt” (P)–alternating pathway for the stages following N_2 binding and H_2 loss, which offers explanations for how the hydrogenated reaction intermediates, diazene and hydrazine, join the N_2 reduction pathway. Key to this issue was the finding that H_2 inhibits the reduction of diazene,¹⁴⁷ but not hydrazine.²¹¹ We took the simplest view, that under turnover, diazene and hydrazine each joins the N_2 reduction pathway at its own characteristic entry point, and each then proceeds to generate both **H** and **I**. As shown in Figure 12, diazene binds to E_2 with the release of H_2 , thereby entering the N_2 pathway as the “final” interconverting form of the E_4 state. N_2H_4 instead binds to E_1 (as proposed for another two-electron substrate, C_2H_2 ^{17,33,103,220}), joining the N_2 pathway with the release of NH_3 to form a stage corresponding to E_7 in the N_2 reduction scheme.¹⁵⁶

7. OBLIGATORY EVOLUTION OF H_2 IN NITROGEN FIXATION: REDUCTIVE ELIMINATION OF H_2

The E_n assignments of Figure 6 plus those of Figure 12 give proposed structures to all E_n states of the LT kinetic scheme (Figure 3), but the assignments have been developed through independent analyses of the two four-electron halves of the eight-electron catalytic cycle (eq 1). In the first half (part I) of the pathway, accumulation of four electrons/protons activates FeMo-co, generating E_4 ; in the second half (part II), bound N_2 is hydrogenated by two of those electrons/protons plus an additional four electrons/protons. However, the assignments are silent about the mechanism by which the E_4 Janus intermediate, Figure 4, connects these two halves: the

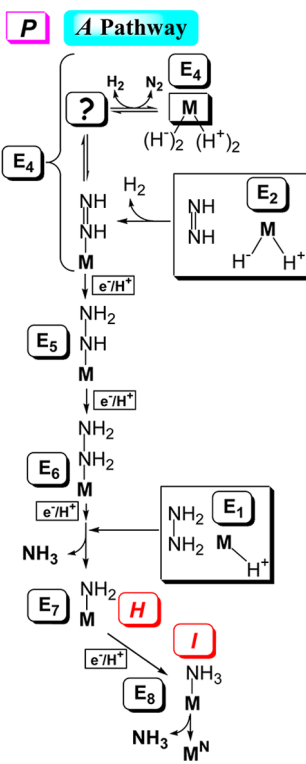


Figure 12. Integration of LT kinetic scheme with “prompt” (P) alternating (A) pathway for N_2 reduction. The ? represents the product of N_2 binding with H_2 release, whose identity is discussed below. Also shown is how diazene and hydrazine join the N_2 reduction pathway. Note: M denotes FeMo-co in its entirety, and substrate-derived species are drawn to indicate stoichiometry only, not mode of substrate binding. E_n states, $n = \text{even}$, are Kramers states; $n = \text{odd}$ are non-Kramers. M^N denotes resting-state FeMo-co. Individual charges on M and a substrate fragment, not shown, sum to the charge on resting FeMo-co. Adapted with permission from ref 156 with corrections based on the re mechanism for H_2 loss upon N_2 binding discussed below. Copyright 2013 American Chemical Society.

obligatory production of an H₂ molecule upon N₂ binding, as shown in Figure 12.^{33,156,158} Why nitrogenase should “waste” fully 25% of the ATP required for nitrogen fixation through H₂ generation (eq 1) has remained a mystery, and indeed is not even accepted uniformly.^{23,221}

Consideration of the finding that E₄ stores its four reducing equivalents as two bridging hydrides (Figure 4) within the context of the well-known organometallic chemistries of hydrides^{194,222} and dihydrogen²²³ led us to examine the two alternative mechanisms by which this state might bind and activate N₂ with release of H₂, and proceed to the prompt formation of FeMo-co with a bound diazene-level species (N₂H₂) without additional accumulation of [e⁻/H⁺], as featured in the P–A reaction pathway, Figure 12. In one, H₂ is formed by hydride protonation (hp mechanism), Figure 13, upper; the other forms H₂ through reductive elimination (re),¹⁹⁵ Figure 13, lower. We first describe these two mechanisms, and then show that the re mechanism is operative.

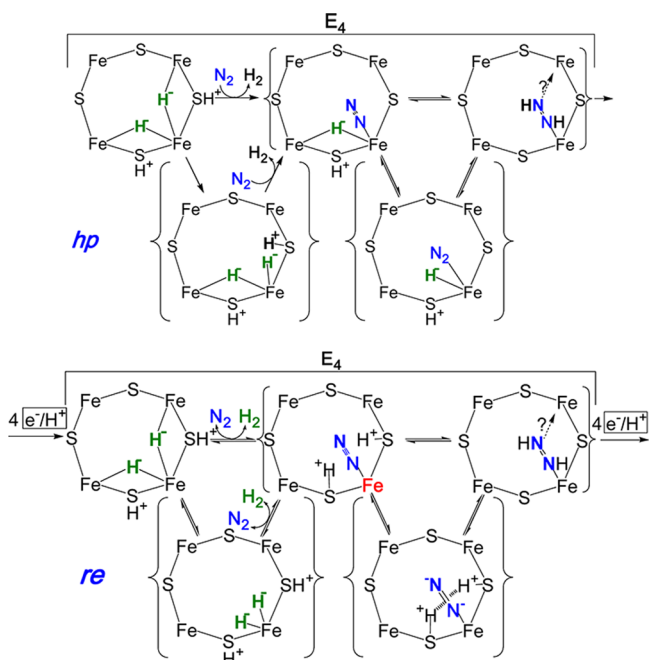


Figure 13. Visualization of hp and re mechanisms for H₂ release upon N₂ (blue) binding to E₄. The following is shown: the Fe-2,3,6,7 face of resting FeMo-co; the structure of FeMo-co must distort in different stages of catalysis. The Fe that binds N₂ is presumed to be Fe6, as indicated by studies of α -70^{Val} variants; when bold, red, Fe6 is formally reduced by two equivalents (see text). The bridging hydrides of E₄ (green) are positioned to share an Fe “vertex”, as suggested by re mechanism of H₂ release upon N₂ binding. Alternative binding modes for N₂-derived species can be envisaged.

7.1. Hydride Protonation (hp) Mechanism

In the hp scheme (Figure 13, upper), N₂ binding is accompanied by the activation of *one* bridging hydride to the terminal form and protonation of this hydride by a sulfide-bound proton to form and release H₂. Such a mechanism for H₂ formation is invoked in discussions of hydrogenases,^{223,224} and there is strong precedence for replacement of a metal-bound H₂ with N₂. In this context, by analogy to the mechanism for the (much less demanding) reduction of alkynes/alkenes one might propose that transient terminalization of the “second” hydride would then lead to hydrogenation

and protonation of the bound N₂, to form FeMo-co bound N₂H₂ (see Figure 13, upper, below). For reasons that will become clear below, the hydrogenation of N₂ to form metal bound-N₂H₂ must be reversible.

7.2. Reductive Elimination (re) Mechanism

The second mechanism for H₂ loss upon N₂ binding begins with transient terminalization of *both* E₄ hydrides, Figure 13, lower. This is followed by reductive elimination of H₂ as N₂ binds, steps with considerable precedence.^{4,194,222,223,225} Of key importance, the departing H₂ carries away only two of the four reducing equivalents stored in E₄, while the Fe that binds N₂ becomes highly activated through formal reduction by two equivalents; for example a formal redox state of Fe(II) would be reduced to Fe(0). This delivery of two reducing equivalents to the FeMo-co core which otherwise is reduced by at most one equivalent during electron/proton activation (Figures 6 and 7) would poised the cofactor to deliver the two activating electrons to N₂, whose π acidity could be further enhanced by electrostatic interactions with the two sulfur-bound protons: combined delivery of the two electrons and protons would directly yield cofactor-bound N₂H₂. This amounts to a “push–pull” mechanism for the hydrogenation of N₂, in which the “push” of electrons from the doubly reduced cofactor onto N₂ is enhanced by the electrostatic “pull” of the protons bound to sulfur. As discussed in section 9, below, models of E₄(N₂) constructed by placing N₂ and two protons on the doubly reduced FeMo-co core modeled with its resting-state structure provide a convincing illustration of this mechanism (and other insights, as well). The diminished electron donation to Fe by protonated sulfides would not only facilitate reductive elimination, but also would act to localize the added electrons on the Fe involved, limiting charge delocalization over the rest of the cofactor. This mechanism provides a compelling rationale for obligatory H₂ formation during N₂ reduction: the transient formation of a state in which an electrostatically activated N₂ is bound to a highly activated, doubly reduced site, thereby generating a state optimally activated to carry out the initial hydrogenations of N₂, the most difficult process in N₂ fixation.

7.3. Mechanistic Constraints Reveal That Nitrogenase Follows the re Mechanisms

A clear choice between hp and re mechanisms is achieved by testing them against the numerous constraints that are associated with the reaction of D₂ with the diazene-level E₄(N₂/N₂H₂) state formed when N₂ binds to the cofactor and is reduced. The three principal constraints are listed in Chart 1.

Chart 1

Chart 1: Key Constraints on HD Formation under N₂/D₂:

- (i) **Stoichiometry:** M-N₂ + D₂ + 2H⁺ + 2e \Rightarrow 2HD + M + N₂
- (ii) **Scrambling:** ‘No’ T⁺ released to solvent under T₂
- (iii) **Reduction Stage:** D₂ reacts at ‘N₂H₂’ level

The first test that they provide for a mechanism is that it must accommodate the finding that when nitrogenase turns over in the presence of *both* N₂ and D₂, then two HD are formed through D₂ cleavage and solvent-proton reduction, with the stoichiometry summarized as constraint i of Chart 1.^{17,226–228} Such HD formation *only* occurs in the presence of N₂, and not during reduction of H⁺ or *any* other substrate.^{226,229,230}

The second key constraint and mechanistic test was revealed by Burgess and co-workers 30 years ago; the absence of exchange into solvent of D^+ / T^+ derived from D_2/T_2 gas, Chart 1, constraint ii.²²⁶ When nitrogenase turns over under a mixture of N_2 and T_2 , HT is formed with stoichiometry corresponding to Chart 1, constraint i, *but* during this process only a negligible amount of T^+ is released to solvent ($\sim 2\%$). The third constraint is provided by a later study of α -195^{His}- and α -191^{Gln}-substituted MoFe proteins.¹⁶¹ It provided persuasive evidence that HD formation under N_2/D_2 requires that the enzyme be at least at the E_4 redox level, with a FeMo-co-bound N–N species at the reduction level of N_2H_2 or beyond, corresponding to the third constraint, Chart 1, iii.¹⁶¹ Constraint iii, plus the stoichiometry of HD formation according to constraint i implies a process described as



Thus, N_2H_2 formation is reversible, as shown in Figure 13.

Figure 14, upper, shows that the characteristics of HD formation during turnover under N_2/D_2 cannot be reconciled

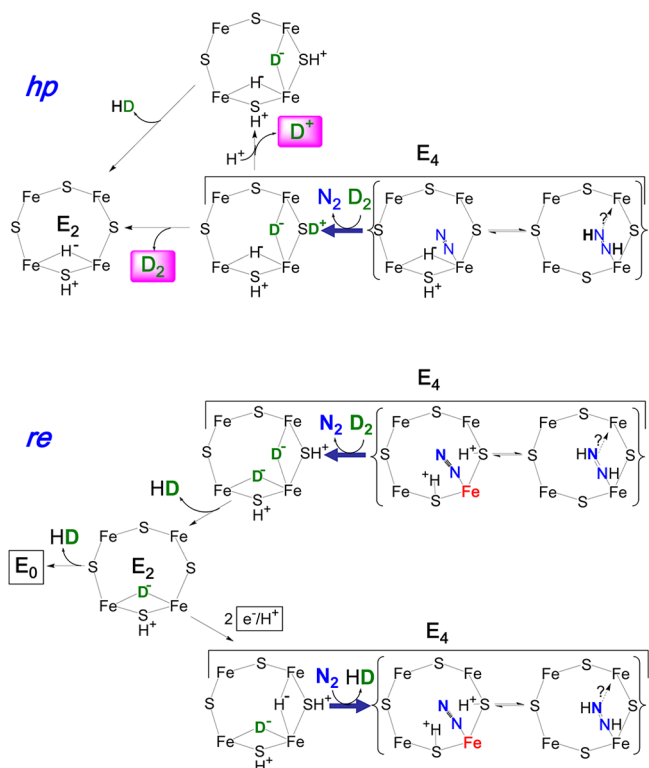


Figure 14. Reversal of hp and re mechanisms upon D_2 binding. Details as in Figure 13. Bold arrows replace equilibrium arrows to emphasize the relaxation process.

with the hp mechanism. In the reverse of this mechanism, D_2 binding and N_2 release would generate an E_4 state that has one deuteride bridge, which is deactivated for exchange with solvent. However, it carries the other deuteron in the form of D^+ bound to sulfur (or a protein residue), which likely would be solvent exchangeable. Exchange of that D^+ would violate the stoichiometric constraint, of eq 3 (line i, Chart 1), as relaxation of E_4 to E_2 within the reverse-hp mechanism would generate only one HD per D_2 , not two as required. Correspondingly, replacement of D_2 by T_2 in Figure 14, upper, with exchange of T^+ bound to sulfide would lose roughly one T^+ per T_2 to

solvent, contrary to the few percent loss observed by Burgess et al. (constraint ii).²²⁶ The possibility that the proton-bearing site is “shielded” from exchange seems implausible for a catalytic cluster that depends on proton delivery for its catalytic function, and in any case solvent exchange need not be fast; the rate-limiting step in nitrogenase turnover is the off-rate for Fe protein after it has delivered its electron to MoFe,^{33,99} and this process is quite slow, with a rate constant of $\sim 6\text{ s}^{-1}$.

If this proton were nonetheless shielded from exchange, relaxation to E_2 would occur with regeneration of D_2 , without the generation of HD, in disagreement with the stoichiometric constraint of Chart 1. This objection would be overcome if at ambient temperatures the hydrides/protons can “migrate” over the FeMo-co face, but this instead would require multiple sites to be “shielded” for slow exchange, while FeMo-co is accessible to rapid proton delivery. Overall, we conclude that the hp process fails to satisfy the constraints of Chart 1, as the reverse hp process satisfies *neither* the stoichiometry of eq 3 nor the constraint that T^+ is not released to solvent (Chart 1).

In contrast, in the reverse of the re mechanism, shown in Figure 14, lower, D_2 binding and N_2 release would generate $E_4(2D)$, the E_4 isotopomer in which *both* atoms of D_2 exist as deuteride bridges. This state would relax with loss of HD to $E_2(D)$, and then to E_0 with loss of the second HD, thus satisfying the stoichiometry of eq 3. If the reaction were carried out under T_2 , essentially no T^+ would be lost to solvent because the bridging deuterides are deactivated for exchange with the protein environment and solvent, thus satisfying the “ T^+ exchange” constraint, Chart 1.

One alternative fate of the $E_4(2D)$ formed by D_2 replacement of N_2 would be to rebind an N_2 , but this would merely release the D_2 that had started the reverse process, creating a cycle invisible to detection. As a second alternative, $E_2(D)$ could acquire two additional electrons/protons to achieve the monodeutero E_4 state. However, as shown in Figure 14, lower, if this state then bound N_2 it would release the second HD, again without solvent exchange, whereas if it ultimately relaxed to E_0 it would release the second HD along with an H_2 . Thus, the re mechanism for N_2 binding and H_2 release not only has the compelling chemical rationale discussed above, but also satisfies the three critical HD constraints for the various alternatives that arise when it is run in reverse, Chart 1.

In short, the re mechanism, Figure 13, lower, satisfies the constraints summarized in Chart 1, as visualized in Figure 14, lower; to the best of our knowledge, it likewise satisfies all other constraints on the mechanism provided by earlier studies, most of which are not directly tied to D_2 binding.

8. TEST OF THE RE MECHANISM

Subsequent to formulation of the re mechanism for the activation of FeMo-cofactor to reduce N_2 (Figure 13, lower),¹⁵⁶ we noted that addition of C_2H_2 to a N_2/D_2 reaction mixture should offer a rigorous test of the mechanism. The test is founded on a defining characteristic of nitrogenase catalysis, an exact distinction between hydrons ($H/D/T$) associated with the gaseous diatomics, $H_2/D_2/T_2$, and those derived from solvent water. Thus, when nitrogenase in protic buffer is turned over under N_2/D_2 , gaseous D_2 can displace N_2 from the $E_4(N_2/N_2H_2)$ state (Figure 14, lower), stoichiometrically yielding two HD.^{226–228} This and other observations clearly show that diatomic H_2/D_2 is not used to reduce N_2 during turnover under $N_2//H_2/D_2$ (in particular, T incorporated into the ammonia product of N_2 fixation would exchange with solvent).¹⁷

Likewise, as demonstrated below, when C_2H_2 is reduced in the presence of D_2 , no deuterated ethylenes are generated.

8.1. Predictions

With this foundation, we recognized that the re mechanism predicts that turnover under $C_2H_2/D_2/N_2$ should not only incorporate H from solvent to generate C_2H_4 by the normal reduction process, but through the agency of the added N_2 also should breach the separation of gaseous D_2 from solvent protons by generating *both* C_2H_3D and $C_2H_2D_2$ (Figure 15).

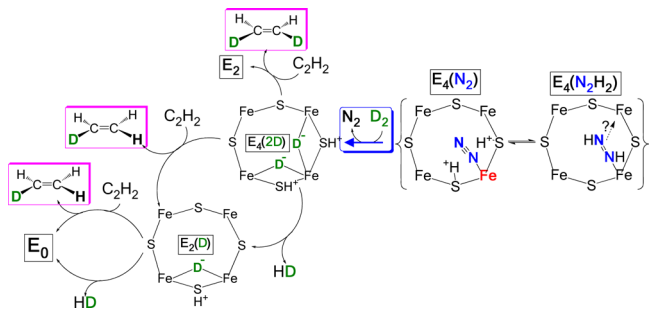


Figure 15. Formation of deuterated acetylenes during turnover under $N_2/D_2/C_2H_2$ as predicted according to the re mechanism. Cartoons again depict the Fe_{2,3,6,7} face of resting-state FeMo-co, with no attempt to incorporate likely structural modifications. Figure shows that the “reverse” of the re mechanism through displacement of N_2 by D_2 produces, successively, $E_4(2D)$ and $E_2(D)$, further showing potential reaction channels for capture of $E_4(2D)$ and $E_2(D)$ intermediates with C_2H_2 .

According to the re mechanism, when turnover is carried out under N_2/D_2 , D_2 can react with $E_4(N_2/N_2H_2)$, replacing the N_2 and undergoing oxidative addition to generate $E_4(2D)$. We recognized that this state in fact might be expected to react with C_2H_2 to form $C_2H_2D_2$ through the idealized mechanism (Figure 16A) involving terminalization of an [Fe–D–Fe] bridge of E_4 , and migratory insertion of bound C_2H_2 into the Fe–D bond to form an Fe-alkenyl intermediate, followed by reductive elimination of $C_2H_2D_2$.^{195,231} Previous studies^{17,103} could not distinguish reaction at the E_4 state from reaction at the E_2 state when C_2H_2 is reduced in the absence of N_2 , as N_2 is required to enable gaseous D_2 to enter the nitrogenase catalytic process. The possibility that acetylene can access different nitrogenase redox states, however, had been suggested on the basis of experiments using a nitrogenase variant that exhibits N_2 reduction that is resistant to inhibition by acetylene.^{232,233}

The $E_4(2D)$ state also would relax through the loss of HD to form $E_2(D)$, an E_2 state whose unique isotopic composition can be generated in no other way. Interception of the $E_2(D)$ state by C_2H_2 would then generate C_2H_3D , with Figure 16B presenting a plausible mechanism: deuteride terminalization and insertion, followed by alkenyl protonolysis.^{195,231} This reaction also might occur through an alternative reaction channel of $E_4(2D)$, as noted in Figure 15.

8.2. Testing the Predictions

We tested the predictions based on the re mechanism of an unprecedented involvement of gaseous D_2 in substrate reduction by use of C_2H_2 reduction under $N_2/D_2/C_2H_2$ gas mixtures to intercept the $E_4(2D)$ and $E_2(D)$ states. As expected, the control reaction of turnover under D_2/C_2H_2 generates only C_2H_4 without incorporation of D from gaseous D_2 to generate either C_2H_3D or $C_2H_2D_2$ (Figure 17). In dramatic contrast,

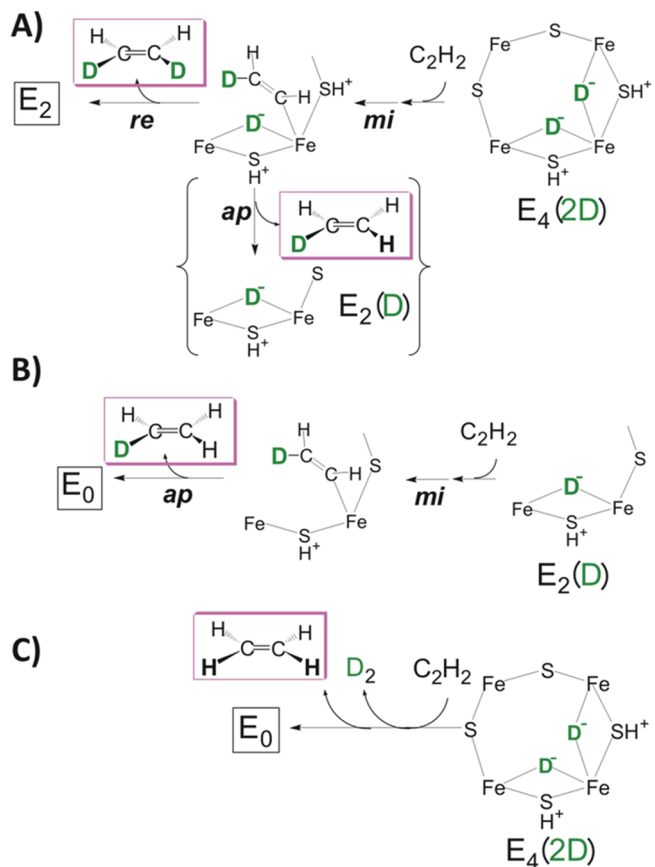


Figure 16. Schematic mechanism for reaction of C_2H_2 with $E_4(2D)$ and $E_2(D)$. (A) Formation of $C_2H_2D_2$, which follows Scheme 15.20 of Hartwig:²³¹ mi = migratory insertion; re = reductive elimination. In braces: Possible alternative reaction channel that leads to formation of C_2H_3D ; ap = alkenyl protonolysis. (B) Schematic mechanism for formation of C_2H_3D from reaction of C_2H_2 with $E_2(D)$. (C) Illustration of possibility that C_2H_2 displaces D_2 formed by reductive elimination of the $E_4(2D)$ deuterides, leading to direct formation of C_2H_4 without D incorporation.

C_2H_2 reduction by nitrogenase under a $N_2/D_2/C_2H_2$ gas mixture in fact produces readily measured amounts of $C_2H_2D_2$ and even greater amounts of C_2H_3D (Figure 17).¹⁵⁷

On reflection, the success of this test for the formation of $E_4(2D)$ is a consequence of the greater reactivity of C_2H_2 compared to that of N_2 and/or of the difference in the likely ways that these two substrates bind to FeMo-co: side-on for C_2H_2 , end-on for N_2 . Otherwise, in a process analogous to that for N_2H_2 formation in the re mechanism (Figure 13, lower), C_2H_2 might in principle displace D_2 formed by reductive elimination of the $E_4(2D)$ deuterides, leading to direct formation of C_2H_4 without D incorporation, Figure 16C. The yield of $C_2H_2D_2$ may be less than that of C_2H_3D , because the contribution from this reaction channel diminishes the yield of the former, but it is perhaps more likely that the binding and reduction of C_2H_2 by $E_4(2D)$ is substantially less likely than the relaxation of $E_4(2D)$ to $E_2(D)$ through loss of HD, and the reduction of C_2H_2 by $E_2(D)$ (Figure 15).

These observations are enriched by consideration of the dependences of the yields of C_2H_3D and $C_2H_2D_2$ on the partial pressures of C_2H_2 , D_2 , N_2 , and electron flux, all of which are understandable in terms of the production of the $E_4(2D)$ and $E_2(D)$ states under these turnover conditions, as predicted by

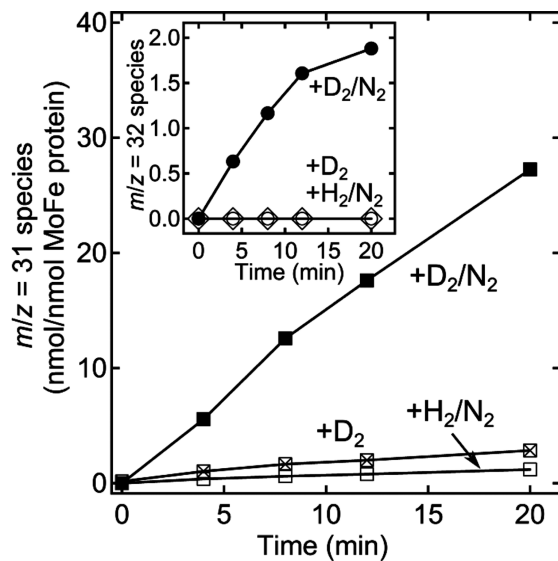
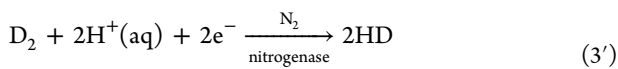


Figure 17. Time-dependent formation of $^{13}\text{C}_2\text{H}_3\text{D}$ and $^{13}\text{C}_2\text{H}_2\text{D}_2$, catalyzed by nitrogenase reduction of $^{13}\text{C}_2\text{H}_2$. $^{13}\text{C}_2\text{H}_3\text{D}$ determined by GC/MS monitoring of $m/z = 31$ for a reaction mixture containing $^{13}\text{C}_2\text{H}_2$ and including D_2 and N_2 (■), just D_2 (x inside □), or H_2 and N_2 (□). Inset: $^{13}\text{C}_2\text{H}_2\text{D}_2$, $m/z = 32$, formation starting with $^{13}\text{C}_2\text{H}_2/\text{D}_2/\text{N}_2$ (●), just D_2 (◊), or H_2/N_2 (○). Partial pressures of 0.02 atm $^{13}\text{C}_2\text{H}_2$, 0.25 atm N_2 , and 0.7 atm H_2/D_2 , where present. The molar ratio of Fe protein to MoFe protein was 2:1. All assays incubated at 30 °C. Adapted with permission from ref 157. Copyright 2013 National Academy of Sciences.

the re mechanism for FeMo-cofactor activation for N_2 binding and reduction.¹⁵⁷ For example, reduction of acetylene and N_2 are mutually exclusive, with complicated inhibition kinetics between these two substrates.^{217,234} Therefore, it was of interest to determine the effect of varying the N_2 partial pressure on the formation of $\text{C}_2\text{H}_3\text{D}$ and $\text{C}_2\text{H}_2\text{D}_2$ at fixed C_2H_2 and D_2 pressures. The yields of $\text{C}_2\text{H}_3\text{D}$ and $\text{C}_2\text{H}_2\text{D}_2$ increase in parallel with increasing partial pressure of N_2 (Figure 18). This can be explained by enhanced formation of $\text{E}_4[\text{N}_2/\text{N}_2\text{H}_2]$ by reaction of N_2 with E_4 . Increased formation of $\text{E}_4[\text{N}_2/\text{N}_2\text{H}_2]$ in turn would enhance reaction with D_2 to form $\text{E}_4(2\text{D})$, which can be intercepted by acetylene to form deuterated ethylenes (Figure 15).¹⁵⁷

It is of interest to note that the reduction of C_2H_2 to $\text{C}_2\text{H}_3\text{D}$ by reaction with $\text{E}_2(\text{D})$ formally corresponds to the reduction of C_2H_2 by the HD that otherwise would form during relaxation of $\text{E}_2(\text{D})$ to E_0 , a perspective that highlights the contrast between this result, achieved in the presence of N_2 , with the failure of nitrogenase to use H_2/D_2 to reduce any substrate in the absence of N_2 . As an elaboration on this perspective, the formation of HD during turnover under N_2/D_2 , with stoichiometry (eq 3, above),¹⁷ can be seen to correspond to the nitrogenase-catalyzed reduction of protons by D_2 and electrons with N_2 as cocatalyst, eq 3'



as the reaction neither proceeds without N_2 nor consumes N_2 . Likewise, although $\text{C}_2\text{H}_2\text{D}_2$ is well-known to form during nitrogenase reduction of C_2D_2 in H_2O buffer (or C_2H_2 in D_2O buffer),¹⁴⁸ formation of this species during turnover under $\text{C}_2\text{H}_2/\text{D}_2/\text{N}_2$ corresponds to the previously unobserved reduction of C_2H_2 by gaseous D_2 with N_2 as cocatalyst (eq 4).

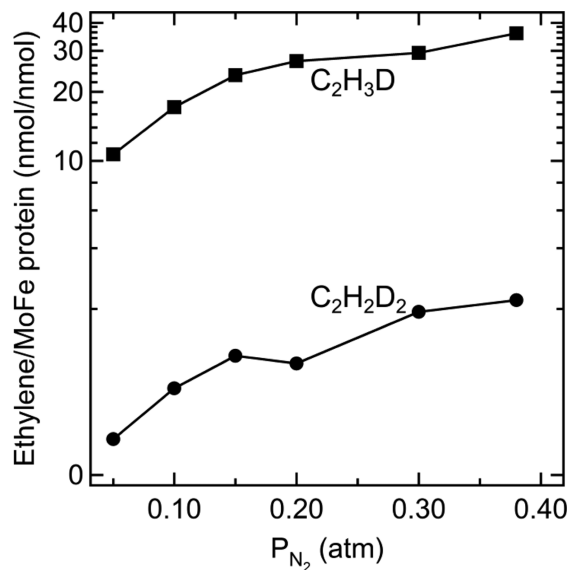
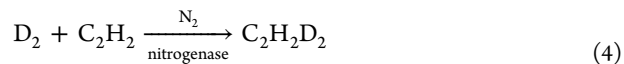


Figure 18. Deuterated ethylene formation as a function of N_2 partial pressure. The partial pressure of C_2H_2 was 0.02 atm and D_2 was 0.6 atm. The molar ratio of Fe protein to MoFe protein was 4:1. Assay conditions as in Figure 17. Adapted with permission from ref 157. Copyright 2013 National Academy of Sciences.



Correspondingly, the formation of $\text{C}_2\text{H}_3\text{D}$ involves incorporation of D^- derived from D_2 along with H^+ from solvent with N_2 as cocatalyst.

9. COMPLETING THE MECHANISM OF NITROGEN FIXATION

Figure 12, above, presents a formal integration of the reaction pathway for nitrogen fixation (intermediates E_4 – E_8) with the LT kinetic scheme, the key to the resulting mechanism being N_2 binding and H_2 release through the re mechanism, Figure 13, lower. This mechanism is built on the structure of the E_4 intermediate and its implication that hydride chemistry is central to nitrogen fixation by nitrogenase (section 3). As a corresponding implication, we further offered the two alternative sets of proposed structures for the “early”, E_1 – E_3 , intermediates (Figure 6). We now discuss in greater depth the E_5 – E_8 intermediates of nitrogen fixation, proposing in Figure 19, II not only more detailed structures for the stages following the formation of N_2H_2 -bound FeMo-co, the $\text{E}_4(\text{N}_2\text{H}_2)$ state, written as binding diazene itself, but also the nature of the chemical transformations that link these stages during the delivery of the ‘second half’ of the eight $[\text{e}^-/\text{H}^+]$ that comprise the stoichiometry of nitrogen fixation, eq 1. The analysis further leads us to provisionally assign the early, “first half” intermediates to the alternative described in Figure 6B, now visualized in Figure 19, I. When combined with the reductive elimination (re) mechanism for the binding N_2 and release of H_2 , Figure 13, lower, the result, Figure 19, is a self-consistent proposal for the structures of all intermediates in the nitrogen fixation mechanism and a formal description of the transformations that convert each stage to the subsequent one: a complete, though of course still simplified, mechanism for nitrogen fixation by nitrogenase.

Figure 19, II, is constructed on two assumptions that (i) the formation and reactions of hydrides is key; (ii) beginning with

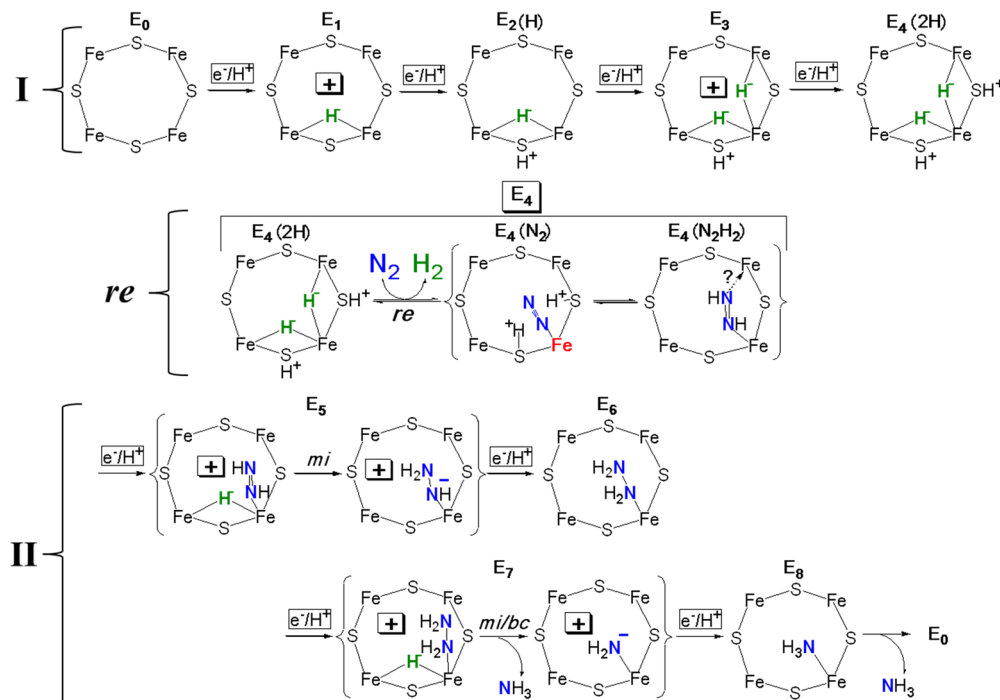


Figure 19. Proposed mechanism displaying structures of all intermediates in nitrogen fixation, inspired by the assumption of primacy of hydride chemistry associated with the Fe_{2,3,6,7} face of FeMo-co, and containing a formal description of the transformations that convert each stage to the subsequent one. In I the mechanism tentatively adopts and visualizes the view of E_n states $n = 1–4$ presented in Figure 6B; in II it visualizes bridging hydrides by analogy, without evidence for or against terminal hydrides for $n = 5–7$. Likewise, the structure of the N_2H_2 species as end-on bound diazene is suggestive, not definitive, etc. I and II are connected by the *re* mechanism, Figure 13, lower. Formal charges are included as useful to help guide the reader.

N_2H_2 , the hydrogenation of reduced forms of N_2 involves migratory insertion into Fe–H bonds. These assumptions lead to the conclusion that $[e^-/H^+]$ transfer to FeMo-co of the $E_4(N_2H_2)$ and E_6 states creates E_5 and E_7 that each contain an [Fe–H–Fe] bridging hydride moiety bound to an oxidized FeMo-co, Figure 19, II, in correspondence with the analogous $[e^-/H^+]$ transfer to E_0 and E_2 , shown in the cartoon of Figure 6B, and now visualized in Figure 19, I. In the case of E_5 , an accompanying migratory insertion of the N_2H_2 into an Fe–H bond (presumably formed by terminalization of the bridge) forms the $[N_2H_3]^-$ moiety bound to the oxidized cluster; in the case of E_7 , migratory insertion leads to N–N bond cleavage and formation of $[NH_2]^-$ bound to the formally oxidized cofactor (Figure 19, II). The follow-up $[e^-/H^+]$ transfer to E_5 , E_7 generates the E_6 and E_8 states, respectively. This mechanistic picture is anchored by the final stages, E_7 and E_8 , whose structures match those proposed in the EPR/ENDOR/ESEEM studies of intermediates H, assigned to E_7 , and I, assigned to E_8 , Figure 12.

The proposal completes a mechanism in which the stoichiometrically required delivery of all 8 $[e^-/H^+]$ to FeMo-co is controlled by the hydride chemistry of the cofactor. The clearly understandable differences between the first “half” of the catalytic cycle, visualized in Figure 19, I, and the “second half”, Figure 19, II, arise because the former involves accumulation of reducing equivalents while the latter involves delivery of reducing equivalents to substrate.

The two halves are similar in that addition of $[e^-/H^+]$ to form an $n = \text{odd}$ intermediate ($n = 1, 3$, first half; $n = 5, 7$, second half) generates an [Fe–H–Fe] bridging hydride attached to a formally oxidized FeMo-co core. They differ in that the hydride is “stored” in $n = 1, 3$, but is promptly

transferred to substrate in $n = 5, 7$ to form a (formally) anionic reduced substrate. Upon addition of $[e^-/H^+]$ to any one of these four $n = \text{odd}$ intermediates, to form the subsequent $n = \text{even}$ intermediate, the electron formally reduces the core to the resting-state redox level. In the first half ($n = 2, 4$), the H^+ is delivered to a sulfur and its charge balances that on a hydride; in the second half ($n = 6, 8$), the proton neutralizes the anionic nitrogenous ligand, to form the neutral, N_2H_4 of E_6 , NH_3 of E_8 .

The two halves of the nitrogen fixation mechanism are joined at the E_4 stage, as described above and displayed as Figure 19, *re*: the $E_4(2H)$ intermediate formed by accumulation of four $[e^-/H^+]$ and containing two bridging hydrides undergoes reductive elimination as it binds N_2 and releases the two “sacrificial” reducing equivalents as H_2 . Figure 19 thus represents a complete mechanism for nitrogen fixation by nitrogenase that invokes the primacy of the hydride chemistry of FeMo-co.

9.1. Uniqueness of N_2 and Nitrogenase

The mechanistic proposal of Figure 19 invokes the primacy of hydride chemistry associated with a 4Fe face of FeMo-co, a structural feature made possible only with a cluster of at least six metal ions. The hydrogenations of reduced forms of N_2 , starting with N_2H_2 , involve migratory insertion of substrate into Fe–H bonds, one at a time. This is the same mechanism visualized for the “normal” reduction of C_2H_2 at the E_2 stage, and even for the rare trapping of E_4 by C_2H_2 , Figure 16; we suggest migratory insertions are likely to be involved in the hydrogenation of all other substrates.

But N_2 is not reactive to hydride insertion. So nitrogenase adopts a different “strategy” for attacking its physiological substrate. It is forced to accumulate four reducing equivalents as

two Fe hydrides, which requires a 4-Fe face, and thus the large cluster is “held together” by the carbide at its core. We have concluded that this cluster can only become activated for N₂ hydrogenation through reductive elimination of two of those equivalents in the form of H₂.^{156,157} The “push” of the doubly reduced metal-ion core of the cluster, compounded by the electrostatic “pull” of sulfur-bound protons, is required to overcome the high barrier to the initial hydrogenation of N₂, directly to N₂H₂, Figure 19.

9.2. Structure of the E₄(N₂) Intermediate: Some Implications

As an exercise to illustrate four points worth noting, we have modeled alternative structures of the E₄(N₂) intermediate by building the bound substrate onto the crystal structure of resting-state FeMo-co using structural information from model complexes.^{235–240} It seems most likely, on the basis of the structures of model complexes, that N₂ binds end-on, rather than bridging. As illustrated in Figure 20, and emphasized over

Second, this mockup demonstrates the commonly understood need for the FeMo-co core to “relax” upon substrate binding. In the resting-state the Fe ions are roughly tetrahedral, and without such relaxation, the N₂–S distances would be far too short. The normal assumption would be that Fe6 roughly forms a plane with three S atoms, with a major contribution to the relaxation being an elongation of the bond *trans* to N₂.

The third issue is the resulting structural/electronic-structure consequences of the *identity* of the *trans* ligand in *exo* versus *endo* N₂ binding, and it does not appear to have been widely discussed. The modulation of metal-ion reactivity by variations in the *trans* ligand (the “*trans* effect”) is well-known,²³¹ and recently, a series of trigonal Fe complexes that are biomimetic of nitrogenase have shown that the *trans* ligands to a terminal Fe–N₂ can regulate the ability of the complex to catalytically reduce N₂.²¹⁴ In the *exo* binding mode, the interstitial carbide is *trans* to N₂. This mode would favor the idea that carbide modulates the properties of Fe6 through the *trans* effect, and may well act as a hemilabile ligand. However, in the *endo* mode, which has been favored by some computations, the *trans* ligand is now a S that bridges to Mo. As C is (roughly) an “in-plane” ligand, not *trans*, its influence on reactivity would be different than for *endo* binding, in which case modulation of Fe6 reactivity by the *trans* effect would involve [S–Mo] being “axial” ligand.

There is a corollary to considerations of the *endo* binding mode. It is widely assumed that the catalytic centers of the alternative nitrogenases have the same structure as FeMo-co, with the heterometal atom Mo being replaced by V or Fe.¹⁸ Thus, if N₂ does bind *endo* to Fe6 of a FeMo-co-like structure in all three systems, its reactivity would be modulated by differences in the axial –S–M “ligand” caused by differences in the properties of Mo, V, and Fe.

The fourth point is the possible importance of interactions of substrate with adjacent amino acid residues. In the *endo* binding mode the N₂ is nestled within a binding pocket capped by the side-chain of α-70^{Val}; in the *exo* mode, the N₂ is pointed to a pocket surrounded by α-191^{Gln} and the homocitrate ligand of Mo. The present mockups suggest that the protein environment in either binding mode could readily accommodate, and even stabilize, N₂ with no more than minor conformational rearrangements.

10. SUMMARY OF MECHANISTIC INSIGHTS

10.1. Catalytic Intermediates of N₂ Fixation

Two major points can be made regarding intermediates trapped: (1) Characterization of the E₄ “Janus” intermediate as bearing four reducing equivalents in the form of two [Fe–H–Fe] bridging hydrides has provided the foundation for proposals that the FeMo-co core is never oxidized or reduced by more than one equivalent relative to the resting-state, and that the oxidative couple in fact is operative, Figure 19, I. (2) The characterization of the common intermediates H and I, trapped during turnover with nitrogenous substrates, led to the proposed unification of kinetic scheme and A reaction pathway, Figure 12.

10.2. re Mechanism

Reductive elimination of two hydrides upon N₂ binding (re mechanism) provides an explanation for the nitrogenase stoichiometry (eq 1) and for the obligatory formation of H₂ upon N₂ binding. This mechanism for H₂ production upon N₂ binding to E₄, Figure 13, lower, satisfies both the stoichiometric

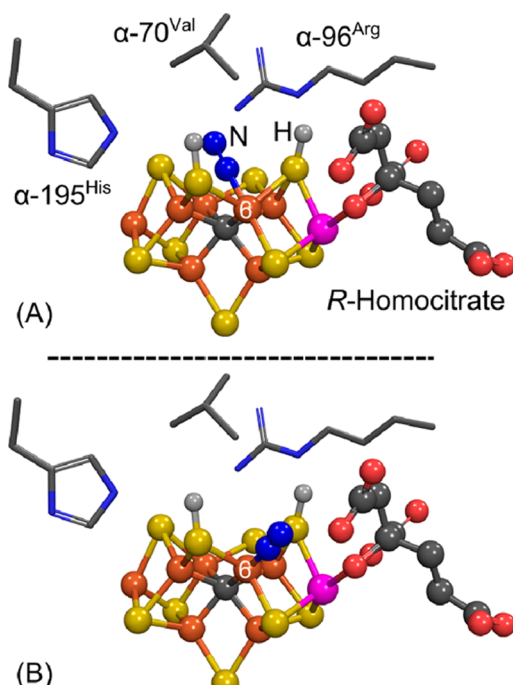


Figure 20. Models for the two alternative modes for N₂ binding at Fe6 of FeMo-cofactor in the E₄(N₂) state, with two protons bound to two adjacent sulfides as in Figure 4: (A) *endo* mode; (B) *exo* mode. The side chains of selected amino acid residues are shown as sticks. The figure was generated in Pymol by building N₂ onto the resting-state of FeMo-co using the coordinate file PDB:2AFK. Iron is shown in rust, molybdenum in magenta, sulfur in yellow, carbon in dark gray, hydrogen in light gray, nitrogen in blue, and oxygen in red.

the years,^{137,241,242} end-on bound N₂ can bind to FeMo-co in two basic, alternative modes: *endo*, with the N₂ “nestled” in the pocket above the Fe2,3,6,7 face; *exo*, with N₂ pointed away from that face. The first point is as follows. According to our mechanism, E₄(N₂) contains doubly reduced metal-ion core with two protons bound to sulfur. There are multiple potential dispositions of the H⁺ on different sulfurs, but distance measurements with the mockups show that the atoms of N₂ and protons can indeed be in close enough proximity to support the electrostatic “pull” postulated above.

constraint of HD formation (Chart 1, line i) and the “T⁺” constraint against exchange of gas-derived hydrons with solvent (Chart 1, line ii), whereas the hp mechanism (Figure 13, upper) satisfies neither. The re mechanism further involves D₂ binding to a state at the “diazene level” of reduction, as required by the constraint of eq 3 and Chart 1, line iii. Finally, to the best of our knowledge, all other constraints on the mechanism, most of which are not directly tied to D₂ binding, are satisfied, as well.

This mechanism answers the following long-standing and oft-repeated question: Why does nature “waste” four ATP/two reducing equivalents through an obligatory loss of H₂ when N₂ binds? The answer follows: reductive elimination of H₂ upon binding of N₂ to FeMo-co of the E₄ state generates a state in which highly reduced FeMo-co binds N₂, which likely is activated for reduction through electrostatic interactions with the remaining two sulfur-bound protons. Transfer of the two reducing equivalents generated by the reductive elimination, combined with transfer of the two activating protons, then forms N₂H₂, Figure 13, lower, in keeping with the P–A scheme of Figure 12. It appears that only through this activation is the enzyme able to hydrogenate N₂.

10.3. Turnover under N₂/D₂/C₂H₂ as a Test of the re Mechanism

This mechanism has been supported by a rigorous test which provided experiments in which C₂H₂ is added to an N₂/D₂ reaction mixture. Although diatomic D₂ does not reduce nitrogenase C₂H₂ in the absence of N₂, the re mechanism successfully predicted that turnover under C₂H₂/D₂/N₂ would breach the separation of gaseous D₂ from solvent protons by generating both C₂H₃D and C₂H₂D₂.

The conclusions regarding H₂ formation upon N₂ binding reached from this study are as follows. (i) The unprecedented incorporation of D from D₂ into the nitrogenase reduction products C₂H₂D₂ and C₂H₃D during turnover under C₂H₂/D₂/N₂ in H₂O demonstrates the presence of the E₄(2D) and E₂(D) states under these conditions. In our view any model that fails to incorporate obligatory H₂ loss as a fundamental aspect of N₂ activation is unlikely to provide a robust description of the chemistry associated with the biological process.²⁴² (ii) This incorporation provides a very clear demonstration of the essential mechanistic role for obligatory, reversible loss of H₂ upon N₂ binding and thus of the eight-electron stoichiometry for nitrogen fixation by nitrogenase embodied in eq 1. Until now, the data indicating that some H₂ must be evolved during N₂ reduction has been viewed as being much more compelling than the data indicating an obligatory evolution of one H₂ for every N₂ reduced, leading to the stoichiometry of eq 1.¹⁷ (iii) The formation of E₄(2D) and E₂(D) during turnover under D₂/N₂ in H₂O is predicted by the re mechanism for the activation of FeMo-cofactor for reduction of N₂, and the interception of these intermediates by C₂H₂ thus provides direct experimental evidence in support of this mechanism (Figure 17). (iv) The well-known reduction of protons by D₂ to form 2HD during turnover under D₂/N₂ in H₂O and the newly discovered reductions of C₂H₂ by D₂/N₂ should be viewed as being catalyzed by nitrogenase with N₂ as cocatalyst. (v) This review has proposed an explanation of the inability of H₂/D₂ to reduce nitrogenase and/or catalyze substrate reduction in the absence of N₂.

11. CONCLUSIONS

The trapping and characterization of five nitrogenase catalytic intermediates, which correspond to three of the five stages involved in binding and reduction of nitrogen (Figure 3), most especially the “Janus intermediate”, E₄, and including the nitrogenous intermediate states H (E₇) and I (E₈), have identified the “prompt–alternating (P–A)” pathway of Figure 12, carried out on a four-Fe face of FeMo-co, as most likely operative for nitrogenase and led to the unification of the nitrogenase reaction pathway and the LT kinetic scheme.

The recognition of the central role played by conversion of accumulated [e⁻/H⁺] into metal hydrides has led to the proposal that this most complex of biological catalytic clusters, and by extension perhaps all biological clusters involved in multielectron substrate hydrogenation, function through a limited set of redox couples, and indeed most likely through a single couple, with multiple reducing equivalents being stored as hydrides rather than as reduced metal ions, Figures 6, 19. Only in this way can a cluster accumulate equivalents delivered at a constant potential set by its biological partners. These considerations provide part of the reason why such a large cluster is required for nitrogenase catalysis.

Simple energetic considerations have further illuminated the heretofore puzzling observation that states of nitrogenase activated by the accumulation of multiple [e⁻/H⁺] can relax through release of H₂ (Scheme 1), but H₂ cannot reduce nitrogenase in what appears to be the reverse process: the answer is that the processes are not microscopic reverses.

Perhaps the central question of nitrogen fixation by nitrogenase has been that of stoichiometry: “Why does (or even, does) nature ‘waste’ four ATP/two reducing equivalents through an obligatory loss of H₂ when N₂ binds?” An answer has been proposed on the basis of further consideration of hydride chemistry exhibited by E₄: the enzyme exhibits the stoichiometry of eq 1 because reductive elimination (re) of two [e⁻/H⁺] in the form of H₂ activates FeMo-co for hydrogenation of N₂ to N₂H₂ via a “push–pull” mechanism, Figure 13, lower. A test of the mechanism involving turnover under N₂/D₂/C₂H₂, as in Figure 15, validated the re mechanism, and in so doing confirmed the stoichiometry of nitrogen fixation, eq 1, as requiring eight [e⁻/H⁺].

The test reaction further highlighted the role of N₂ as cocatalyst in reductions catalyzed by nitrogenase that would not occur in the absence of N₂. We have further noted some issues regarding the uniqueness of N₂ and nitrogenase as the catalyst for its hydrogenation, and of the implications of alternative structures of the N₂ complex.

The result of these efforts is the mechanism for nitrogen fixation presented in Figure 19 for further tests, both experimental and theoretical.

ASSOCIATED CONTENT

Supporting Information

Analysis of the relative orientations of bridging hydrides of E₄ intermediate. This material is available free of charge via the Internet at <http://pubs.acs.org>.

AUTHOR INFORMATION

Corresponding Authors

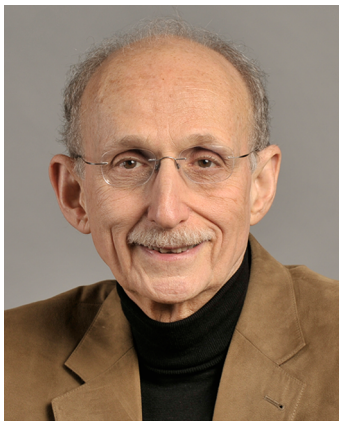
*E-mail: bmh@northwestern.edu.

*E-mail: deandr@vbi.vt.edu.

*E-mail: lance.seefeldt@usu.edu.

Notes

The authors declare no competing financial interest.

Biographies

Brian M. Hoffman was an undergraduate at the University of Chicago, received his Ph.D. from Caltech, and spent a postdoctoral year at MIT. From there, he went to Northwestern University, where he is the Charles E. and Emma H. Morrison Professor in the Departments of Chemistry and of Molecular Biosciences. He is a member of the National Academy of Sciences.



Dmitriy Lukyanov received a M.S. degree and a Ph.D. from Kazan State University. He is a postdoctoral fellow at Northwestern University.



Zhi-Yong Yang received a B.S. degree in chemistry and a Ph.D. degree in organic chemistry from Nankai University in Tianjin, China. Following a position at Shanghai ChemPartner as an organic scientist, he joined the Ph.D. program in biochemistry at Utah State University, where he recently completed his degree. During the past 12 years, his

research has covered biomimetic chemistry of hydrogenases, and the mechanism of nitrogenase. His research interest is in the activation and formation of chemical bonds catalyzed by biological and synthetic transition-metal catalysts.



Dennis R. Dean received a B.A. from Wabash College and a Ph.D. from Purdue University. He is currently a University Distinguished Professor at Virginia Tech where he also serves as the Director of the Fralin Life Science Institute and the Virginia Bioinformatics Institute.



Lance C. Seefeldt received a B.S. degree in chemistry from the University of Redlands in California and a Ph.D. in biochemistry from the University of California at Riverside. He was a postdoctoral fellow at the Center for Metalloenzyme Studies at the University of Georgia before joining the faculty of the Chemistry and Biochemistry Department at Utah State University, where he is now Professor. He was recently awarded the D. Wynne Thorne Career Research Award and elected a Fellow of the American Association for the Advancement of Science. Over the past 25 years, his research has focused on elucidating the mechanism of nitrogenase.

ACKNOWLEDGMENTS

This work was supported by the NIH (HL 13531, B.M.H.; GM59087, L.C.S. and D.R.D.), NSF (MCB 0723330, B.M.H.), and DOE (DE-SC0010687 to L.C.S. and D.R.D.). We gratefully acknowledge many illuminating discussions with friends and colleagues, most especially noting Professors Richard H. Holm, Pat Holland, and Jonas Peters. Thanks to Dr. K. Danyal for assistance with Figure 1.

REFERENCES

- (1) Ferguson, S. J. *Curr. Opin. Chem. Biol.* **1998**, 2, 182.
- (2) Smil, V. *Enriching the Earth: Fritz Haber, Carl Bosch, and the Transformation of World Food Production*; MIT Press: Cambridge, MA, 2004.

- (3) Jia, H.-P.; Quadrelli, E. A. *Chem. Soc. Rev.* **2014**, *43*, 547.
- (4) MacKay, B. A.; Fryzuk, M. D. *Chem. Rev.* **2004**, *104*, 385.
- (5) Canfield, D. E.; Glazer, A. N.; Falkowski, P. G. *Science* **2010**, *330*, 192.
- (6) Cheng, Q. *J. Integr. Plant Biol.* **2008**, *50*, 786.
- (7) Thamdrup, B. *Annu. Rev. Ecol. Evol. Syst.* **2012**, *43*, 407.
- (8) Raymond, J.; Siefert, J. L.; Staples, C. R.; Blankenship, R. E. *Mol. Biol. Evol.* **2004**, *21*, 541.
- (9) Gruber, N.; Galloway, J. N. *Nature* **2008**, *451*, 293.
- (10) Burk, D. *Ergeb. Enzymforsch.* **1934**, *3*, 23.
- (11) Burk, D.; Lineweaver, H.; Horner, C. K. *J. Bacteriol.* **1934**, *27*, 325.
- (12) McGlynn, S. E.; Boyd, E. S.; Peters, J. W.; Orphan, V. J. *Front. Microbiol.* **2013**, *3*, 419.
- (13) Dos Santos, P. C.; Fang, Z.; Mason, S. W.; Setubal, J. C.; Dixon, R. *BMC Genomics* **2012**, *13*, 162.
- (14) Haber, F. *Naturwissenschaften* **1922**, *10*, 1041.
- (15) Haber, F. *Naturwissenschaften* **1923**, *11*, 339.
- (16) Boyd, E. S.; Anbar, A. D.; Miller, S.; Hamilton, T. L.; Lavin, M.; Peters, J. W. *Geobiology* **2011**, *9*, 221.
- (17) Burgess, B. K.; Lowe, D. J. *Chem. Rev.* **1996**, *96*, 2983.
- (18) Eady, R. R. *Chem. Rev.* **1996**, *96*, 3013.
- (19) Beatty, P. H.; Good, A. G. *Science* **2011**, *333*, 416.
- (20) Godfray, H. C. J.; Beddington, J. R.; Crute, I. R.; Haddad, L.; Lawrence, D.; Muir, J. F.; Pretty, J.; Robinson, S.; Thomas, S. M.; Toulmin, C. *Science* **2010**, *327*, 812.
- (21) Rubio, L. M.; Ludden, P. W. *Annu. Rev. Microbiol.* **2008**, *62*, 93.
- (22) Macleod, K. C.; Holland, P. L. *Nat. Chem.* **2013**, *5*, 559.
- (23) Peters, J. C.; Mehn, M. P. In *Activation of Small Molecules: Organometallic and Bioinorganic Perspectives*; Tolman, W. B., Ed.; Wiley-VCH Verlag GmbH & Co. KGaA: Weinheim, Germany, 2006; pp 81–119.
- (24) Schrock, R. R. *Acc. Chem. Res.* **2005**, *38*, 955.
- (25) Tanabe, Y.; Nishibayashi, Y. *Coord. Chem. Rev.* **2013**, *257*, 2551.
- (26) Jodin, C. C. R. *Acad. Paris* **1862**, *55*, 612.
- (27) Carnahan, J. E.; Mortenson, L. E.; Mower, H. F.; Castle, J. E. *Biochim. Biophys. Acta* **1960**, *44*, 520.
- (28) Bulen, W. A.; Burns, R. C.; LeComte, J. R. *Biochem. Biophys. Res. Commun.* **1964**, *17*, 265.
- (29) Schneider, K. C.; Bradbeer, C.; Singh, R. N.; Wang, L. C.; Wilson, P. W.; Burris, R. H. *Proc. Natl. Acad. Sci. U.S.A.* **1960**, *46*, 726.
- (30) Burgess, B. K. *Chem. Rev.* **1990**, *90*, 1377.
- (31) Hardy, R. W.; Burns, R. C.; Parshall, G. W. In *Bioinorganic Chemistry*; Dessy, R., Dillard, J., Taylor, L., Eds.; American Chemical Society: Washington, DC, 1971; Vol. 100, pp 219–247.
- (32) Howard, J. B.; Rees, D. C. *Chem. Rev.* **1996**, *96*, 2965.
- (33) Thorneley, R. N. F.; Lowe, D. J. In *Molybdenum Enzymes*; Spiro, T. G., Ed.; Wiley: New York, 1985; pp 221–284.
- (34) Winter, H. C.; Burris, R. H. *Annu. Rev. Biochem.* **1976**, *45*, 409.
- (35) Bulen, W. A.; LeComte, J. R. *Proc. Natl. Acad. Sci. U.S.A.* **1966**, *56*, 979.
- (36) Mortenson, L. E. *Fed. Proc.* **1965**, *24*, 233.
- (37) Mortenson, L. E. *Biochim. Biophys. Acta* **1966**, *127*, 18.
- (38) Hageman, R. V.; Burris, R. H. *Proc. Natl. Acad. Sci. U.S.A.* **1978**, *75*, 2699.
- (39) Dean, D. R.; Bolin, J. T.; Zheng, L. *J. Bacteriol.* **1993**, *175*, 6737.
- (40) Howard, J. B.; Rees, D. C. *Annu. Rev. Biochem.* **1994**, *63*, 235.
- (41) Kim, J.; Rees, D. C. *Biochemistry* **1994**, *33*, 389.
- (42) Bulen, W. A.; Burns, R. C.; LeComte, J. R. *Proc. Natl. Acad. Sci. U.S.A.* **1965**, *53*, 532.
- (43) Burns, R. C.; Bulen, W. A. *Biochim. Biophys. Acta* **1965**, *105*, 437.
- (44) Mortenson, L. E. *Biochim. Biophys. Acta* **1964**, *81*, 473.
- (45) Mortenson, L. E. *Proc. Natl. Acad. Sci. U.S.A.* **1964**, *52*, 272.
- (46) Shah, V. K.; Brill, W. J. *Proc. Natl. Acad. Sci. U.S.A.* **1977**, *74*, 3249.
- (47) Peters, J. W.; Fisher, K.; Newton, W. E.; Dean, D. R. *J. Biol. Chem.* **1995**, *270*, 27007.
- (48) Kim, J.; Rees, D. C. *Science* **1992**, *257*, 1677.
- (49) Ma, L.; Brosius, M. A.; Burgess, B. K. *J. Biol. Chem.* **1996**, *271*, 10528.
- (50) Lowe, D. J.; Fisher, K.; Thorneley, R. N. F. *Biochem. J.* **1993**, *292*, 93.
- (51) Georgiadis, M. M.; Komiya, H.; Chakrabarti, P.; Woo, D.; Kornuc, J. J.; Rees, D. C. *Science* **1992**, *257*, 1653.
- (52) Kim, J.; Rees, D. C. *Nature* **1992**, *360*, 553.
- (53) Chan, M. K.; Kim, J.; Rees, D. C. *Science* **1993**, *260*, 792.
- (54) Kim, J.; Woo, D.; Rees, D. C. *Biochemistry* **1993**, *32*, 7104.
- (55) Jang, S. B.; Seefeldt, L. C.; Peters, J. W. *Biochemistry* **2000**, *39*, 14745.
- (56) Jang, S. B.; Seefeldt, L. C.; Peters, J. W. *Biochemistry* **2000**, *39*, 641.
- (57) Jang, S. B.; Jeong, M. S.; Seefeldt, L. C.; Peters, J. W. *J. Biol. Inorg. Chem.* **2004**, *9*, 1028.
- (58) Jeong, M. S. *Mol. Cells* **2004**, *18*, 374.
- (59) Strop, P.; Takahara, P. M.; Chiu, H.-J.; Angove, H. C.; Burgess, B. K.; Rees, D. C. *Biochemistry* **2001**, *40*, 651.
- (60) Sen, S.; Igashira, R.; Smith, A.; Johnson, M. K.; Seefeldt, L. C.; Peters, J. W. *Biochemistry* **2004**, *43*, 1787.
- (61) Sen, S.; Krishnakumar, A.; McClead, J.; Johnson, M. K.; Seefeldt, L. C.; Szilagyi, R. K.; Peters, J. W. *J. Inorg. Biochem.* **2006**, *100*, 1041.
- (62) Peters, J. W.; Stowell, M. H. B.; Soltis, S. M.; Finnegan, M. G.; Johnson, M. K.; Rees, D. C. *Biochemistry* **1997**, *36*, 1181.
- (63) Mayer, S. M.; Lawson, D. M.; Gormal, C. A.; Roe, S. M.; Smith, B. E. *J. Mol. Biol.* **1999**, *292*, 871.
- (64) Sørlie, M.; Christiansen, J.; Lemon, B. J.; Peters, J. W.; Dean, D. R.; Hales, B. *J. Biochemistry* **2001**, *40*, 1540.
- (65) Einsle, O.; Tezcan, F. A.; Andrade, S. L. A.; Schmid, B.; Yoshida, M.; Howard, J. B.; Rees, D. C. *Science* **2002**, *297*, 1696.
- (66) Schmid, B.; Ribbe, M. W.; Einsle, O.; Yoshida, M.; Thomas, L. M.; Dean, D. R.; Rees, D. C.; Burgess, B. K. *Science* **2002**, *296*, 352.
- (67) Rees, D. C.; Tezcan, F. A.; Haynes, C. A.; Walton, M. Y.; Andrade, S.; Einsle, O.; Howard, J. B. *Phil. Trans. R. Soc., A* **2005**, *363*, 971.
- (68) Sarma, R.; Mulder, D. W.; Brecht, E.; Szilagyi, R. K.; Seefeldt, L. C.; Tsuruta, H.; Peters, J. W. *Biochemistry* **2007**, *46*, 14058.
- (69) Sarma, R.; Barney, B. M.; Keable, S.; Dean, D. R.; Seefeldt, L. C.; Peters, J. W. *J. Inorg. Biochem.* **2010**, *104*, 385.
- (70) Spatzal, T.; Aksoyoglu, M.; Zhang, L.; Andrade, S. L. A.; Schleicher, E.; Weber, S.; Rees, D. C.; Einsle, O. *Science* **2011**, *334*, 940.
- (71) Lancaster, K. M.; Roemelt, M.; Ettenhuber, P.; Hu, Y.; Ribbe, M. W.; Neese, F.; Bergmann, U.; DeBeer, S. *Science* **2011**, *334*, 974.
- (72) Lancaster, K. M.; Hu, Y.; Bergmann, U.; Ribbe, M. W.; DeBeer, S. *J. Am. Chem. Soc.* **2013**, *135*, 610.
- (73) Wiig, J. A.; Hu, Y.; Lee, C. C.; Ribbe, M. W. *Science* **2012**, *337*, 1672.
- (74) Wiig, J. A.; Lee, C. C.; Hu, Y.; Ribbe, M. W. *J. Am. Chem. Soc.* **2013**, *135*, 4982.
- (75) Lee, H.-I.; Benton, P. M. C.; Laryukhin, M.; Igashira, R. Y.; Dean, D. R.; Seefeldt, L. C.; Hoffman, B. M. *J. Am. Chem. Soc.* **2003**, *125*, 5604.
- (76) Yang, T.-C.; Maeser, N. K.; Laryukhin, M.; Lee, H.-I.; Dean, D. R.; Seefeldt, L. C.; Hoffman, B. M. *J. Am. Chem. Soc.* **2005**, *127*, 12804.
- (77) Lukyanov, D.; Pelmenschikov, V.; Maeser, N.; Laryukhin, M.; Yang, T. C.; Noodlemen, L.; Dean, D. R.; Case, D. A.; Seefeldt, L. C.; Hoffman, B. M. *Inorg. Chem.* **2007**, *46*, 11437.
- (78) Chiu, H.-J.; Peters, J. W.; Lanzilotta, W. N.; Ryle, M. J.; Seefeldt, L. C.; Howard, J. B.; Rees, D. C. *Biochemistry* **2001**, *40*, 641.
- (79) Schmid, B.; Einsle, O.; Chiu, H.-J.; Willing, A.; Yoshida, M.; Howard, J. B.; Rees, D. C. *Biochemistry* **2002**, *41*, 15557.
- (80) Schindelin, H.; Kisker, C.; Schlessman, J. L.; Howard, J. B.; Rees, D. C. *Nature* **1997**, *387*, 370.
- (81) Tezcan, F. A.; Kaiser, J. T.; Mustafi, D.; Walton, M. Y.; Howard, J. B.; Rees, D. C. *Science* **2005**, *309*, 1377.
- (82) Soboh, B.; Boyd, E. S.; Zhao, D.; Peters, J. W.; Rubio, L. M. *FEBS Lett.* **2010**, *584*, 1487.

- (83) Dos Santos, P. C.; Dean, D. R.; Hu, Y.; Ribbe, M. W. *Chem. Rev.* **2004**, *104*, 1159.
- (84) Hu, Y.; Fay, A. W.; Lee, C. C.; Yoshizawa, J.; Ribbe, M. W. *Biochemistry* **2008**, *47*, 3973.
- (85) Hu, Y.; Ribbe, M. W. *Acc. Chem. Res.* **2010**, *43*, 475.
- (86) Hu, Y.; Ribbe, M. W. *Microbiol. Mol. Biol. Rev.* **2011**, *75*, 664.
- (87) Hu, Y.; Ribbe, M. W. *Coord. Chem. Rev.* **2011**, *255*, 1218.
- (88) Hu, Y.; Ribbe, M. W. *J. Biol. Chem.* **2013**, *288*, 13173.
- (89) Hu, Y.; Ribbe, M. W. *Biochim. Biophys. Acta* **2013**, *1827*, 1112.
- (90) Rehder, D. J. *Inorg. Biochem.* **2000**, *80*, 133.
- (91) Eady, R. R. *Coord. Chem. Rev.* **2003**, *237*, 23.
- (92) Crans, D. C.; Smee, J. J.; Gaidamauskas, E.; Yang, L. *Chem. Rev.* **2004**, *104*, 849.
- (93) Fisher, K.; Dilworth, M. J.; Newton, W. E. *Biochemistry* **2006**, *45*, 4190.
- (94) Lee, C. C.; Hu, Y.; Ribbe, M. W.; Holm, R. H. *Proc. Natl. Acad. Sci. U.S.A.* **2009**, *106*, 9209.
- (95) Lee, C. C.; Hu, Y.; Ribbe, M. W. *Science* **2010**, *329*, 642.
- (96) Lee, C. C.; Hu, Y.; Ribbe, M. W. *Angew. Chem., Int. Ed.* **2011**, *50*, 5545.
- (97) Dance, I. *Dalton Trans.* **2011**, *40*, 5516.
- (98) Hu, Y.; Lee, C. C.; Ribbe, M. W. *Dalton Trans.* **2012**, *41*, 1118.
- (99) Duval, S.; Danyal, K.; Shaw, S.; Lytle, A. K.; Dean, D. R.; Hoffman, B. M.; Antony, E.; Seefeldt, L. C. *Proc. Natl. Acad. Sci. U.S.A.* **2013**, *110*, 16414.
- (100) Seefeldt, L. C.; Hoffman, B. M.; Dean, D. R. *Curr. Opin. Chem. Biol.* **2012**, *16*, 19.
- (101) Howard, J. B.; Rees, D. C. *Proc. Natl. Acad. Sci. U.S.A.* **2006**, *103*, 17088.
- (102) Duyvis, M. G.; Wassink, H.; Haaker, H. *Biochemistry* **1998**, *37*, 17345.
- (103) Wilson, P. E.; Nyborg, A. C.; Watt, G. D. *Biophys. Chem.* **2001**, *91*, 281.
- (104) Peters, J. W.; Szilagyi, R. K. *Curr. Opin. Chem. Biol.* **2006**, *10*, 101.
- (105) Danyal, K.; Mayweather, D.; Dean, D. R.; Seefeldt, L. C.; Hoffman, B. M. *J. Am. Chem. Soc.* **2010**, *132*, 6894.
- (106) Danyal, K.; Dean, D. R.; Hoffman, B. M.; Seefeldt, L. C. *Biochemistry* **2011**, *50*, 9255.
- (107) Mayweather, D.; Danyal, K.; Dean, D. R.; Seefeldt, L. C.; Hoffman, B. M. *Biochemistry* **2012**, *51*, 8391.
- (108) Chan, J. M.; Christiansen, J.; Dean, D. R.; Seefeldt, L. C. *Biochemistry* **1999**, *38*, 5779.
- (109) Nyborg, A. C.; Johnson, J. L.; Gunn, A.; Watt, G. D. *J. Biol. Chem.* **2000**, *275*, 39307.
- (110) Rupnik, K.; Hu, Y.; Lee, C. C.; Wiig, J. A.; Ribbe, M. W.; Hales, B. J. *J. Am. Chem. Soc.* **2012**, *134*, 13749.
- (111) Lanzilotta, W. N.; Christiansen, J.; Dean, D. R.; Seefeldt, L. C. *Biochemistry* **1998**, *37*, 11376.
- (112) Duyvis, M. G.; Wassink, H.; Haaker, H. *FEBS Lett.* **1996**, *380*, 233.
- (113) Angove, H. C.; Yoo, S. J.; Münck, E.; Burgess, B. K. *J. Biol. Chem.* **1998**, *273*, 26330.
- (114) Seefeldt, L. C.; Dean, D. R. *Acc. Chem. Res.* **1997**, *30*, 260.
- (115) Chan, J. M.; Ryle, M. J.; Seefeldt, L. C. *J. Biol. Chem.* **1999**, *274*, 17593.
- (116) Lanzilotta, W. N.; Parker, V. D.; Seefeldt, L. C. *Biochim. Biophys. Acta* **1999**, *1429*, 411.
- (117) Ryle, M. J.; Seefeldt, L. C. *J. Biol. Chem.* **2000**, *275*, 6214.
- (118) Danyal, K.; Inglet, B. S.; Vincent, K. A.; Barney, B. M.; Hoffman, B. M.; Armstrong, F. A.; Dean, D. R.; Seefeldt, L. C. *J. Am. Chem. Soc.* **2010**, *132*, 13197.
- (119) Roth, L. E.; Nguyen, J. C.; Tezcan, F. A. *J. Am. Chem. Soc.* **2010**, *132*, 13672.
- (120) Roth, L. E.; Tezcan, F. A. *ChemCatChem* **2011**, *3*, 1549.
- (121) Roth, L. E.; Tezcan, F. A. *J. Am. Chem. Soc.* **2012**, *134*, 8416.
- (122) Durrant, M. C. *Biochem. J.* **2001**, *355*, 569.
- (123) Durrant, M. C. *Biochemistry* **2002**, *41*, 13934.
- (124) Durrant, M. C. *Biochemistry* **2002**, *41*, 13946.
- (125) Cui, Z.; Dunford, A. J.; Durrant, M. C.; Henderson, R. A.; Smith, B. E. *Inorg. Chem.* **2003**, *42*, 6252.
- (126) Thorneley, R. N. F.; Angove, H. C.; Durrant, M. C.; Fairhurst, S. A.; George, S. J.; Sinclair, A.; Tolland, J. D.; Hallenbeck, P. C. *J. Inorg. Biochem.* **2003**, *96*, 18.
- (127) Durrant, M. C.; Francis, A.; Lowe, D. J.; Newton, W. E.; Fisher, K. *Biochem. J.* **2006**, *397*, 261.
- (128) Hinnemann, B.; Nørskov, J. K. *J. Am. Chem. Soc.* **2003**, *125*, 1466.
- (129) Hinnemann, B.; Nørskov, J. K. *J. Am. Chem. Soc.* **2004**, *126*, 3920.
- (130) Hinnemann, B.; Nørskov, J. K. *Phys. Chem. Chem. Phys.* **2004**, *6*, 843.
- (131) Hinnemann, B.; Nørskov, J. K. *Top. Catal.* **2006**, *37*, 55.
- (132) Varley, J. B.; Nørskov, J. K. *ChemCatChem* **2013**, *5*, 732.
- (133) Lovell, T.; Li, J.; Liu, T.; Case, D. A.; Noodleman, L. *J. Am. Chem. Soc.* **2001**, *123*, 12392.
- (134) Lovell, T.; Liu, T.; Case, D. A.; Noodleman, L. *J. Am. Chem. Soc.* **2003**, *125*, 8377.
- (135) Torres, R. A.; Lovell, T.; Noodleman, L.; Case, D. A. *J. Am. Chem. Soc.* **2003**, *125*, 1923.
- (136) Pelmenschikov, V.; Case, D. A.; Noodleman, L. *Inorg. Chem.* **2008**, *47*, 6162.
- (137) Dance, I. *J. Am. Chem. Soc.* **2007**, *129*, 1076.
- (138) Harris, T. V.; Szilagyi, R. K. *Inorg. Chem.* **2011**, *50*, 4811.
- (139) Neese, F. *Angew. Chem., Int. Ed.* **2006**, *45*, 196.
- (140) Kästner, J.; Blöchl, P. E. *J. Am. Chem. Soc.* **2007**, *129*, 2998.
- (141) Seefeldt, L. C.; Rasche, M. E.; Ensign, S. A. *Biochemistry* **1995**, *34*, 5382.
- (142) Rasche, M. E.; Seefeldt, L. C. *Biochemistry* **1997**, *36*, 8574.
- (143) Mayer, S. M.; Niehaus, W. G.; Dean, D. R. *J. Chem. Soc., Dalton Trans.* **2002**, 802.
- (144) Dos Santos, P. C.; Mayer, S. M.; Barney, B. M.; Seefeldt, L. C.; Dean, D. R. *J. Inorg. Biochem.* **2007**, *101*, 1642.
- (145) Igarashi, R. Y.; Dos Santos, P. C.; Niehaus, W. G.; Dance, I. G.; Dean, D. R.; Seefeldt, L. C. *J. Biol. Chem.* **2004**, *279*, 34770.
- (146) Dos Santos, P. C.; Igarashi, R. Y.; Lee, H.-I.; Hoffman, B. M.; Seefeldt, L. C.; Dean, D. R. *Acc. Chem. Res.* **2005**, *38*, 208.
- (147) Barney, B. M.; McClead, J.; Lukyanov, D.; Laryukhin, M.; Yang, T.-C.; Dean, D. R.; Hoffman, B. M.; Seefeldt, L. C. *Biochemistry* **2007**, *46*, 6784.
- (148) Seefeldt, L. C.; Yang, Z.-Y.; Duval, S.; Dean, D. R. *Biochim. Biophys. Acta* **2013**, *1827*, 1102.
- (149) Fisher, K.; Dilworth, M. J.; Kim, C.-H.; Newton, W. E. *Biochemistry* **2000**, *39*, 10855.
- (150) Yang, Z.-Y.; Dean, D. R.; Seefeldt, L. C. *J. Biol. Chem.* **2011**, *286*, 19417.
- (151) Hu, Y.; Lee, C. C.; Ribbe, M. W. *Science* **2011**, *333*, 753.
- (152) Yang, Z.-Y.; Moure, V. R.; Dean, D. R.; Seefeldt, L. C. *Proc. Natl. Acad. Sci. U.S.A.* **2012**, *109*, 19644.
- (153) Barney, B. M.; Lee, H.-I.; Dos Santos, P. C.; Hoffman, B. M.; Dean, D. R.; Seefeldt, L. C. *Dalton Trans.* **2006**, 2277.
- (154) Seefeldt, L. C.; Hoffman, B. M.; Dean, D. R. *Annu. Rev. Biochem.* **2009**, *78*, 701.
- (155) Hoffman, B. M.; Dean, D. R.; Seefeldt, L. C. *Acc. Chem. Res.* **2009**, *42*, 609.
- (156) Hoffman, B. M.; Lukyanov, D.; Dean, D. R.; Seefeldt, L. C. *Acc. Chem. Res.* **2013**, *46*, 587.
- (157) Yang, Z.-Y.; Khadka, N.; Lukyanov, D.; Hoffman, B. M.; Dean, D. R.; Seefeldt, L. C. *Proc. Natl. Acad. Sci. U.S.A.* **2013**, *110*, 16327.
- (158) Simpson, F. B.; Burris, R. H. *Science* **1984**, *224*, 1095.
- (159) Davis, L. C.; Henzl, M. T.; Burris, R. H.; Orme-Johnson, W. H. *Biochemistry* **1979**, *18*, 4860.
- (160) Barney, B. M.; Laryukhin, M.; Igarashi, R. Y.; Lee, H.-I.; Dos Santos, P. C.; Yang, T.-C.; Hoffman, B. M.; Dean, D. R.; Seefeldt, L. C. *Biochemistry* **2005**, *44*, 8030.
- (161) Fisher, K.; Dilworth, M. J.; Newton, W. E. *Biochemistry* **2000**, *39*, 15570.

- (162) Scott, D. J.; May, H. D.; Newton, W. E.; Brigle, K. E.; Dean, D. R. *Nature* **1990**, *343*, 188.
- (163) Thomann, H.; Bernardo, M.; Newton, W. E.; Dean, D. R. *Proc. Natl. Acad. Sci. U.S.A.* **1991**, *88*, 6620.
- (164) Kim, C.-H.; Newton, W. E.; Dean, D. R. *Biochemistry* **1995**, *34*, 2798.
- (165) Dilworth, M. J.; Fisher, K.; Kim, C.-H.; Newton, W. E. *Biochemistry* **1998**, *37*, 17495.
- (166) Barney, B. M.; Lukoyanov, D.; Igarashi, R. Y.; Laryukhin, M.; Yang, T.-C.; Dean, D. R.; Hoffman, B. M.; Seefeldt, L. C. *Biochemistry* **2009**, *48*, 9094.
- (167) Benton, P. M. C.; Laryukhin, M.; Mayer, S. M.; Hoffman, B. M.; Dean, D. R.; Seefeldt, L. C. *Biochemistry* **2003**, *42*, 9102.
- (168) Lee, H.-I.; Igarashi, R. Y.; Laryukhin, M.; Doan, P. E.; Dos Santos, P. C.; Dean, D. R.; Seefeldt, L. C.; Hoffman, B. M. *J. Am. Chem. Soc.* **2004**, *126*, 9563.
- (169) Igarashi, R. Y.; Laryukhin, M.; Dos Santos, P. C.; Lee, H.-I.; Dean, D. R.; Seefeldt, L. C.; Hoffman, B. M. *J. Am. Chem. Soc.* **2005**, *127*, 6231.
- (170) Barney, B. M.; Yang, T.-C.; Igarashi, R. Y.; Dos Santos, P. C.; Laryukhin, M.; Lee, H.-I.; Hoffman, B. M.; Dean, D. R.; Seefeldt, L. C. *J. Am. Chem. Soc.* **2005**, *127*, 14960.
- (171) Barney, B. M.; Lukoyanov, D.; Yang, T.-C.; Dean, D. R.; Hoffman, B. M.; Seefeldt, L. C. *Proc. Natl. Acad. Sci. U.S.A.* **2006**, *103*, 17113.
- (172) Orme-Johnson, W. H.; Hamilton, W. D.; Jones, T. L.; Tso, M. Y. W.; Burris, R. H.; Shah, V. K.; Brill, W. J. *Proc. Natl. Acad. Sci. U.S.A.* **1972**, *69*, 3142.
- (173) Hoffman, B. M. *J. Phys. Chem.* **1994**, *98*, 11657.
- (174) Hoffman, B. M.; Sturgeon, B. E.; Doan, P. E.; DeRose, V. J.; Liu, K. E.; Lippard, S. J. *J. Am. Chem. Soc.* **1994**, *116*, 6023.
- (175) Hoffman, B. M. *Proc. Natl. Acad. Sci. U.S.A.* **2003**, *100*, 3575.
- (176) Hoffman, B. M. *Acc. Chem. Res.* **2003**, *36*, 522.
- (177) Schweiger, A.; Jeschke, G. *Principles of Pulse Electron Paramagnetic Resonance*; Oxford University Press: Oxford, U.K., 2001.
- (178) George, S. J.; Barney, B. M.; Mitra, D.; Igarashi, R. Y.; Guo, Y.; Dean, D. R.; Cramer, S. P.; Seefeldt, L. C. *J. Inorg. Biochem.* **2012**, *112*, 85.
- (179) Huynh, B. H.; Henzl, M. T.; Christner, J. A.; Zimmermann, R.; Orme-Johnson, W. H.; Münck, E. *Biochim. Biophys. Acta* **1980**, *623*, 124.
- (180) Yoo, S. J.; Angove, H. C.; Papaefthymiou, V.; Burgess, B. K.; Münck, E. *J. Am. Chem. Soc.* **2000**, *122*, 4926.
- (181) Lowe, D. J.; Eady, R. R.; Thorneley, N. F. *Biochem. J.* **1978**, *173*, 277.
- (182) Fisher, K.; Newton, W. E.; Lowe, D. J. *Biochemistry* **2001**, *40*, 3333.
- (183) Lukoyanov, D.; Barney, B. M.; Dean, D. R.; Seefeldt, L. C.; Hoffman, B. M. *Proc. Natl. Acad. Sci. U.S.A.* **2007**, *104*, 1451.
- (184) Barney, B. M.; Igarashi, R. Y.; Dos Santos, P. C.; Dean, D. R.; Seefeldt, L. C. *J. Biol. Chem.* **2004**, *279*, 53621.
- (185) Yates, M. G.; Lowe, D. J. *FEBS Lett.* **1976**, *72*, 121.
- (186) Kinney, R. A.; Hetterscheid, D. G. H.; Hanna, B. S.; Schrock, R. R.; Hoffman, B. M. *Inorg. Chem.* **2010**, *49*, 704.
- (187) Willems, J.-P.; Lee, H.-I.; Burdi, D.; Doan, P. E.; Stubbe, J.; Hoffman, B. M. *J. Am. Chem. Soc.* **1997**, *119*, 9816.
- (188) Kinney, R. A.; Saouma, C. T.; Peters, J. C.; Hoffman, B. M. *J. Am. Chem. Soc.* **2012**, *134*, 12637.
- (189) Lukoyanov, D.; Yang, Z.-Y.; Dean, D. R.; Seefeldt, L. C.; Hoffman, B. M. *J. Am. Chem. Soc.* **2010**, *132*, 2526.
- (190) Henderson, R. A. *Chem. Rev.* **2005**, *105*, 2365.
- (191) Henderson, R. A. *Coord. Chem. Rev.* **2005**, *249*, 1841.
- (192) Chiang, K. P.; Scarborough, C. C.; Horitani, M.; Lees, N. S.; Ding, K.; Dugan, T. R.; Brennessel, W. W.; Bill, E.; Hoffman, B. M.; Holland, P. L. *Angew. Chem., Int. Ed.* **2012**, *51*, 3658.
- (193) Doan, P. E.; Telser, J.; Barney, B. M.; Igarashi, R. Y.; Dean, D. R.; Seefeldt, L. C.; Hoffman, B. M. *J. Am. Chem. Soc.* **2011**, *133*, 17329.
- (194) Peruzzini, M.; Poli, R. *Recent Advances in Hydride Chemistry*; Elsevier Science B.V.: Amsterdam, The Netherlands, 2001.
- (195) Crabtree, R. H. *The Organometallic Chemistry of the Transition Metals*, 5th ed.; Wiley: Hoboken, NJ, 2009.
- (196) Oro, L. A.; Sola, E. In *Recent Advances in Hydride Chemistry*; Peruzzini, M.; Poli, R., Eds.; Elsevier Science B.V.: Amsterdam, The Netherlands, 2001; pp 299–328.
- (197) Zimmermann, R.; Münck, E.; Brill, W. J.; Shah, V. K.; Henzl, M. T.; Rawlings, J.; Orme-Johnson, W. H. *Biochim. Biophys. Acta* **1978**, *537*, 185.
- (198) Lee, H.-I.; Sørlie, M.; Christiansen, J.; Yang, T.-C.; Shao, J.; Dean, D. R.; Hales, B. J.; Hoffman, B. M. *J. Am. Chem. Soc.* **2005**, *127*, 15880.
- (199) Siegbahn, P. E. M.; Tye, J. W.; Hall, M. B. *Chem. Rev.* **2007**, *107*, 4414.
- (200) Surawatanawong, P.; Hall, M. B. *Inorg. Chem.* **2010**, *49*, 5737.
- (201) Pickett, C. J. *J. Biol. Inorg. Chem.* **1996**, *1*, 601.
- (202) Chatt, J.; Dilworth, J. R.; Richards, R. L. *Chem. Rev.* **1978**, *78*, 589.
- (203) Chatt, J.; Richards, R. L. *J. Organomet. Chem.* **1982**, *239*, 65.
- (204) Schrock, R. R. *Chem. Commun.* **2003**, 2389.
- (205) Yandulov, D. V.; Schrock, R. R. *Science* **2003**, *301*, 76.
- (206) Schrock, R. R. *Angew. Chem., Int. Ed.* **2008**, *47*, 5512.
- (207) Lukoyanov, D.; Dikanov, S. A.; Yang, Z.-Y.; Barney, B. M.; Samoilova, R. I.; Narasimhulu, K. V.; Dean, D. R.; Seefeldt, L. C.; Hoffman, B. M. *J. Am. Chem. Soc.* **2011**, *133*, 11655.
- (208) Thorneley, R. N.; Lowe, D. J. *Biochem. J.* **1984**, *224*, 887.
- (209) Burgess, B. K. In *Metal Ions in Biology: Molybdenum Enzymes*; Spiro, T. G., Ed.; John Wiley and Sons: New York, 1985; pp 161–220.
- (210) Thorneley, R. N. F.; Eady, R. R.; Lowe, D. J. *Nature* **1978**, *272*, 557.
- (211) Davis, L. C. *Arch. Biochem. Biophys.* **1980**, *204*, 270.
- (212) Murakami, J.; Yamaguchi, W. *Sci. Rep.* **2012**, *2*, 407.
- (213) Rodriguez, M. M.; Bill, E.; Brennessel, W. W.; Holland, P. L. *Science* **2011**, *334*, 780.
- (214) Anderson, J. S.; Rittle, J.; Peters, J. C. *Nature* **2013**, *501*, 84.
- (215) Dilworth, M. J.; Eady, R. R. *Biochem. J.* **1991**, *277*, 465.
- (216) McKenna, C. E.; Simeonov, A. M.; Eran, H.; Bravo-Leerabhandh, M. *Biochemistry* **1996**, *35*, 4502.
- (217) Seefeldt, L. C.; Dance, I. G.; Dean, D. R. *Biochemistry* **2004**, *43*, 1401.
- (218) Müncck, E.; Ksurerus, K.; Hendrich, M. P. *Metallobiochemistry Part D: Physical and Spectroscopic Methods for Probing Metal Ion Environment in Metalloproteins*. In *Methods in Enzymology*; James, F., Riordan, B. L. V., Ed.; Academic Press: New York, 1993; Vol. 227, pp 463–479.
- (219) Lukoyanov, D.; Yang, Z.-Y.; Barney, B. M.; Dean, D. R.; Seefeldt, L. C.; Hoffman, B. M. *Proc. Natl. Acad. Sci. U.S.A.* **2012**, *109*, 5583.
- (220) Lowe, D. J.; Fisher, K.; Thorneley, R. N. *Biochem. J.* **1990**, *272*, 621.
- (221) As summarized by Peters and Mehn, many of the attempts to understand nitrogen fixation theoretically treat a six-electron stoichiometry, and thus implicitly reject this central mechanistic feature of the LT scheme.
- (222) Ballmann, J.; Munhá, R. F.; Fryzuk, M. D. *Chem. Commun.* **2010**, *46*, 1013.
- (223) Kubas, G. J. *Chem. Rev.* **2007**, *107*, 4152.
- (224) Tard, C.; Pickett, C. J. *Chem. Rev.* **2009**, *109*, 2245.
- (225) Crabtree, R. H. *Inorg. Chim. Acta* **1986**, *125*, L7.
- (226) Burgess, B. K.; Wherland, S.; Newton, W. E.; Stiefel, E. I. *Biochemistry* **1981**, *20*, 5140.
- (227) Li, J.-L.; Burris, R. H. *Biochemistry* **1983**, *22*, 4472.
- (228) Jensen, B. B.; Burris, R. H. *Biochemistry* **1985**, *24*, 1141.
- (229) Hoch, G. E.; Schneider, K. C.; Burris, R. H. *Biochim. Biophys. Acta* **1960**, *37*, 273.
- (230) Jackson, E. K.; Parshall, G. W.; Hardy, R. W. F. *J. Biol. Chem.* **1968**, *243*, 4952.
- (231) Hartwig, J. *Organotransition Metal Chemistry: From Bonding to Catalysis*; University Science Books: Sausalito, CA, 2010.

- (232) Christiansen, J.; Seefeldt, L. C.; Dean, D. R. *J. Biol. Chem.* **2000**, *275*, 36104.
- (233) Christiansen, J.; Cash, V. L.; Seefeldt, L. C.; Dean, D. R. *J. Biol. Chem.* **2000**, *275*, 11459.
- (234) Rivera-Ortiz, J. M.; Burris, R. H. *J. Bacteriol.* **1975**, *123*, 537.
- (235) Stieber, S. C. E.; Milsmann, C.; Hoyt, J. M.; Turner, Z. R.; Finkelstein, K. D.; Wieghardt, K.; DeBeer, S.; Chirik, P. J. *Inorg. Chem.* **2012**, *51*, 3770.
- (236) Moret, M.-E.; Peters, J. C. *J. Am. Chem. Soc.* **2011**, *133*, 18118.
- (237) Moret, M.-E.; Peters, J. C. *Angew. Chem., Int. Ed.* **2011**, *50*, 2063.
- (238) Saouma, C. T.; Moore, C. E.; Rheingold, A. L.; Peters, J. C. *Inorg. Chem.* **2011**, *50*, 11285.
- (239) Takaoka, A.; Mankad, N. P.; Peters, J. C. *J. Am. Chem. Soc.* **2011**, *133*, 8440.
- (240) Fong, H.; Moret, M.-E.; Lee, Y.; Peters, J. C. *Organometallics* **2013**, *32*, 3053.
- (241) Dance, I. *Chem.—Asian J.* **2007**, *2*, 936.
- (242) Dance, I. *Chem. Commun.* **2013**, *49*, 10893.